Journal of Medicinal Chemistry



Article

# Discovery, Optimization, and Biological Evaluation of 5-(2-(trifluoromethyl)phenyl)-indazoles as a Novel Class of Transient Receptor Potential A1 (TRPA1) Antagonists

Lisa Rooney, Agnès Vidal, Anne-Marie D'Souza, Nick Devereux, Brian Masick, Valerie Boissel, Ryan West, Victoria Head, Rowan Stringer, Jianmin Lao, Matt J Petrus, Ardem Patapoutian, Mark Nash, Natalie Stoakley, Moh Panesar, J Martin Verkuyl, Andrew M Schumacher, H. Michael Petrassi, and David C. Tully

*J. Med. Chem.*, **Just Accepted Manuscript** • DOI: 10.1021/jm401986p • Publication Date (Web): 02 Jun 2014

# Discovery, Optimization, and Biological Evaluation of 5-(2-(trifluoromethyl)phenyl)-indazoles as a Novel Class of Transient Receptor Potential A1 (TRPA1) Antagonists

*Lisa Rooney,[‡] Agnès Vidal,[†] Anne-Marie D'Souza,[‡] Nick Devereux,[‡] Brian Masick,[†] Valerie Boissel,[‡] Ryan West,[‡] Victoria Head,[‡] Rowan Stringer,[‡] Jianmin Lao,[†] Matt J. Petrus,[†] Ardem Patapoutian,[†] Mark Nash,[‡] Natalie Stoakley,[‡] Moh Panesar,[‡] J. Martin Verkuyl,[‡] Andrew M. Schumacher[†], H. Michael Petrassi,[†] and David C. Tully*[†]*

[†]Genomics Institute of the Novartis Research Foundation, 10675 John Jay Hopkins Drive, San Diego, California 92121, United States

[‡]Novartis Institutes for Biomedical Research, Wimblehurst Road, Horsham RH12 5AB, United Kingdom

**RECEIVED DATE**

ABSTRACT. A high throughput screening campaign identified 5-(2-chlorophenyl)-indazole Compound **4** as an antagonist of the Transient Receptor Potential A1 (TRPA1) ion channel with $IC_{50}$=1.23 μM. Hit to lead medicinal chemistry optimization established the SAR around the

indazole ring system, demonstrating that a trifluoromethyl group at the 2-position of the phenyl ring in combination with various substituents at the 6-position of the indazole ring greatly contributed to improvements *in vitro* activity. Further lead optimization resulted in the identification of Compound **31**, a potent and selective antagonist of TRPA1 *in vitro* ($IC_{50}$ = 0.015 μM), which has moderate oral bioavailability in rodents and demonstrates robust activity *in vivo* in several rodent models of inflammatory pain.

KEYWORDS. TRPA1 antagonist, ANKTM1, transient receptor potential ion channel, inflammatory pain, visceral pain

## INTRODUCTION

Transient Receptor Potential A1 (TRPA1) is a non-selective cation channel that functions as a polymodal sensory receptor and plays an important role in nociception, or the sensing of noxious stimuli. The channel is expressed in sensory neurons, particularly within the dorsal root ganglia (DRG), and in the visceral tissues such as the small intestine, colon, bladder, and stomach.[1-4] TRPA1 is activated by $Ca^{2+}$,[5,6] cold temperatures,[3] inflammatory peptides,[7] and naturally occurring electrophilic compounds such as allyl isothiocyanate (AITC), cinnamaldehyde, and allicin, which covalently modify the protein and result in the channel opening.[6,8,9] TRPA1 activation by these agents likely accounts for the pungent sensation elicited by foods such as garlic, horseradish, and wasabi. In addition, TRPA1 activation in sensory neurons results in secretion of pro-inflammatory peptides such as substance P and calcitonin gene-related peptide (CGRP), which both play a role in pain transmission from the DRG neurons.[3,7,10,11] TRPA1 signaling is believed to play a role in nociception involving neuropathic

pain resulting from injury or disease, as well as visceral pain stemming from underlying gastrointestinal disease or urinary bladder dysfunction.[12]

Human genetics further support a role for TRPA1 in pain. A gain of function mutation in TRPA1 has been linked to Familial Episodic Pain Syndrome (FEPS), and patients carrying this mutation experience episodes of excruciating pain, mainly in the abdominal region, which are triggered by fasting, cold, or physical exercise.[13] Conversely, TRPA1 knockout mice show a reduced pain response to TRPA1 agonists, including inflammatory mediators such as 4-hydroxynonenal.[8,14-17] This evidence suggests that TRPA1 may be responsible for transmitting pain signals and that antagonizing its calcium channel activity may be a useful approach for the treatment of pain.[18,19]

There have been only a few classes of TRPA1 antagonists reported in the literature to date:[18-20] oximes such as AP-18 (**1**)[21] and A-967079 (**2**)[22,23] and xanthines such as HC-030031 (**3**)[24,25], although there are several additional scaffold classes which have been claimed in patents applications and subsequently evaluated in recent review articles.[19,26,27] Consistent with the TRPA1 knockout mouse findings, **2** and **3** exhibited analgesic effects in rodent pain models in response to sensitization induced by mustard oil.[23,24] Furthermore, oral administration of **3** was shown to reduce Complete Freund's Adjuvant (CFA)-induced inflammatory pain, as well as neuropathic pain caused by spinal nerve ligation in rats.[24] Taken together, these genetic and pharmacological results suggest the potential utility of antagonizing TRPA1 to treat pain. However, the relatively low potency of **3** ($IC_{50}$ = 2.3 μM) and poor *in vivo* pharmacokinetics of **2** (high Cl, short $T_{1/2}$ in rodents) leave plenty of room for the optimization of potent TRPA1 antagonists with improved *in vivo* pharmacokinetics that would better suited for further pharmaceutical development.

Herein we report the discovery and SAR surrounding a novel scaffold class of TRPA1 antagonists derived from 5-phenyl indazole. Compound **4** was originally identified in a high-throughput screening (HTS) campaign of our proprietary compound collection. We initiated medicinal chemistry on this scaffold with the primary objectives of improving *in vitro* potency and *in vivo* PK, and our efforts have resulted in a novel series of potent TRPA1 antagonists with potent activity *in vivo* in rodent models of inflammatory pain.

## Chemistry

The 5-phenyl indazoles could all be synthesized using a Suzuki palladium catalyzed cross-coupling reaction to form the biaryl scaffold (Scheme 1). The reaction of unprotected 5-bromo indazole (**6a)** with commercially available boronic acids proceeded to give sufficient yields of many of the desired products shown in Table 1. Where the aryl boronic acids were not available, the alternative coupling of *tert*-butyl-5-(4,4,5,5-tetramethyl-1,3,2-dioxaborolan-2-yl)-1H-indazole-1-carboxylate (**9**) with the aryl bromide provided the products in a single step as the protecting group was lost under the reaction conditions.

For the investigation of the effect of substitution on the indazole ring, the 5-bromo indazoles required were synthesized from their corresponding 4-bromo-2-methylaniline (**5**). Route A provided acetyl protected indazoles which were taken into the Suzuki cross-coupling step. The acetyl protecting group was not stable under the Suzuki conditions, and in the absence of a protecting group on the indazole, the competing debromination reaction tended to become more prevalent. The rate of the cross coupling versus the deacetylation varied due to the nature of the R group, and therefore a more stable protecting group was desired. Route B provided the unprotected indazoles in good yields and a THP group was then introduced prior to the Suzuki

reaction. Following the completion of this work it has been noted that conditions have now been reported to allow the Suzuki-type cross coupling of unprotected indazoles and other azoles to proceed with high yields.[28]

Late stage functionalization from the common ester intermediate **10h** was used to access **35**, **40** and **42** (Scheme 2). Reduction to the alcohol **45** and alkylation using methyl iodide, followed by removal of the THP protecting group provided **40**. Oxidation of alcohol **45** with manganese dioxide and treatment with DAST introduced the $CF_2H$ group. Hydrolysis of the ester **10h** and amide formation via the acid chloride allowed access to amide derivative **44**.

The intermediate **10d**, also used in the synthesis of **36** could be further transformed to the 6-cyclopropyl derivative **34** (Scheme 3). Deprotection of the aryl methyl ether and formation of the aryl triflate **51** allowed for Suzuki coupling with cyclopropyl boronic acid to introduce the alkyl substituent.

## Results and Discussion

As part of our efforts to discover novel chemical scaffolds that could inhibit TRPA1 activation, a high throughput screen (HTS) of our compound collection was conducted on approximately 1.8 M compounds using an antagonist mode FLIPR $Ca^{2+}$ imaging assay in 1536-well format. Compound **4** was identified as a primary hit in this HTS using selection criteria of >50% inhibition at 10 μM. Following the hit-pick and reconfirmation assay, compound **4** was shown to have $IC_{50}$ = 1.23 μM with 91% inhibition of TRPA1 activation by cinnamaldehyde. Indazole **4** was considered to be a particularly attractive starting point for medicinal chemistry optimization due to its relative drug-likeness based on calculated parameters such as low molecular weight

(MW = 228 Da), number of rotatable bonds (=1), number of hydrogen bond donors (=1), and number of hydrogen bond acceptors (=2).

During our initial exploration of the SAR of this scaffold, we first evaluated the effect of the phenyl substituent by directly replacing the chlorine on compound **4** with other substituents. Replacement of the chlorine with hydrogen (compound **11**) results in complete loss of activity, while the fluoro analog **12** was a weak, partial blocker of TRPA1 activation. The SAR of the phenyl ring demonstrates sensitivity toward the size of the alkyl substituent in that ethyl and isopropyl groups are fairly well tolerated (compounds **14** and **15**, respectively), while a methyl group (compound **13**) or a tert-butyl group (compound **16**) results in a significant loss of potency. Following the SAR at the ortho position of the phenyl ring, the trifluoromethyl group was then explored in compound **17** ($IC_{50}$ = 0.164 μM). The favorable steric and unique inductive electron-withdrawing properties of the trifluoromethyl group ultimately turned out to be the most preferred substituent as reflected by the order of magnitude improvement in potency from the original hit compound **4**. The SAR around this position proved to be quite steep as exemplified by loss of potency by subtle changes to compound **17** such as replacing fluorine with hydrogen, as in the difluoromethyl analog **18**, or inserting oxygen, as in the trifluoromethoxy analog **19**. A similar loss in potency was also observed with the small polar nitrile group (compound **20**) despite the strong electron withdrawing nature of this substituent.

Prior to embarking on more extensive lead optimization efforts, we investigated whether this indazole scaffold was able to block TRPA1 activation by different chemical agonists. In addition to cinnemaldehyde, the TRPA1 agonist used in our primary FLIPR assay (at $EC_{80}$ concentration), compound **17** was able to effectively block TRPA1 activation by a variety of other agonists, including AITC and also the highly potent agonist dibenzo[b,f][1,4]oxazepine-4-

carboxamide, previously described by Gijsen, et. al.[29] As shown in Table 4, $IC_{50}$ values for blocking TRPA1 activation are similar (roughly within three-fold) with different chemical agonists, each with effectively complete inhibition. This attribute was reassuring, and based on our internal experience with this and other scaffolds suggested that this indazole series of antagonists would likely have the ability to block TRPA1 activation regardless of the nature of activating stimuli.

In continuation of our lead optimization efforts from compound **17**, we next chose to explore whether additional substituents were permitted at any other position of the phenyl ring or around the indazole ring with the optimal $CF_3$ group in place. In consideration of the initial SAR for this scaffold which was quite steep, we set out to introduce subtle changes by strategically installing either fluorine or a methyl group around the phenyl indazole ring system in order to learn which positions would tolerate or benefit from substituents (Table 2). Neither the 3- nor 4-positions of the phenyl ring tolerated the addition of fluorine as demonstrated by compounds **21** and **22**, while the 5-fluoro and 6-fluoro analogs (**23** and **24**) resulted in a loss of activity. Substitution of the indazole ring with fluorine demonstrated subtle effects, with the 4-fluoroindazole analog (**25**) losing twofold in potency over **17**, while installation of a fluorine at the indazole 6-position affords a threefold improvement in potency (compound **26**). Since the incorporation of methyl groups to either the 3- or 7-positions of the indazole resulted in a steep loss of activity (compounds **27** and **28**), we chose to focus our efforts on the indazole 6-position for further exploration of the SAR of this scaffold.

The SAR of 6-substituted indazole analogs is described in Table 3, with each of the analogs bearing the requisite trifluoromethyl group at the *ortho* position of the phenyl ring. In general small, hydrophobic substituents tend to improve the potency, while hydrophobic groups with

larger steric demands tend to result in a significant loss of activity. The more optimal substituents were found to be chloro (compound **30**) and small alkyl (Me, Et) or alkyl ethers (MeO, EtO, $CF_3O$) resulting in potent *in vitro* activities with $IC_{50}$ values generally below 50 nM. Interestingly, while the 6-*iso*-propyl analog is nearly inactive (compound **33**), the cyclopropyl remains quite potent (compound **34**). Likewise a similar trend is observed for isopropoxy (**38**, $IC_{50}$ = 0.970 μM) versus cyclopropylmethyloxy (**39**, $IC_{50}$ = 0.026 μM). Both of these observations further demonstrate the subtleties of the steric and electronic demands in this region of the scaffold. Small polar substituents such as a nitrile are tolerated (**43**), but do not confer any improvement in potency over the lead compound **17**. In contrast, larger polar substituents are not tolerated, particularly when bearing a hydrogen bond donor, such as simple amides exemplified by compound **44**.

In advance of selecting compounds for evaluation in preclinical rodent models, several of the more potent analogs were tested *in vitro* against rat and mouse TRPA1 in order to determine the extent of species cross-reactivity (Table 5). There have been previous reports demonstrating species-specific differential pharmacology, whereby antagonists of human TPRA1 exhibit agonist activities at rat and/or mouse TRPA1 homologs.[6,30,31] As outlined in Table 5, most compounds tend to exhibit on average a three-fold to five-fold drop off in activity between hTRPA1 and either rTRPA1 or mTRPA1, with some wider variances. In general, both rat and mouse TRPA1 homologs appear to be less tolerant of the larger substituents at the 6-position of the indazole ring, and as such the sterically less demanding hydrophobic substituents such as methyl (**31**) and chloro (**30**) tended to be more potent *in vitro* against rat and mouse TRPA1. Furthermore, as shown in Table 4, compound **31** was also highly effective at blocking TRPA1

activation by multiple agonists, which proved to be a consistent trend with this indazole scaffold class of TRPA1 antagonists.

We also tested this subset of analogs against several related thermo-TRP channels that have been shown to play a role in the transduction of nociceptive pain, including the vanilloid receptors TRPV1 and TRPV3, as well as the cold and menthol receptor TRPM8. As shown in Table 5, this series of indazoles displays only weak or partial antagonist activity towards each of the TRP channels tested, each with greater than 100-fold window of selectivity over TRPA1. Potent, antagonist activity towards TRPA1 across multiple species and against multiple agonists, combined with a favorable selectivity profile over related thermo-TRP channels provided confidence that observed analgesic activity in vivo would be mediated through TRPA1 directly. Additionally, as the indazole is a common hinge-binding motif found in kinase inhibitors, we tested compounds **17**, **30**, **31**, and **36** across our in-house panel of kinases, and no inhibitory activity was observed below 10 μM.

The *in vivo* pharmacokinetic properties in male Wistar rats selected indazole analogs are summarized in Table 6. Single dose intravenous PK demonstrated that the volumes of distribution for most analogs from this series tend to remain consistently within the moderate range of 1.6 – 3.6 L/kg, while the nature of the substituent at the 6-position of the indazole ring had a significant influence on the *in vivo* clearance rates. Analogs **17** and **30**, with hydrogen and chlorine, respectively, had relatively low clearance, while the substituents that are more prone to oxidative metabolism such as methyl (**31**) and ethers (**36** and **39**) lead to relatively higher *in vivo* clearance and shorter $T_{1/2}$ in the rat. Oral pharmacokinetics were studied using a 10 mg/kg dose administered from a 0.5% methylcelluose/0.5% Tween80 aqueous suspension formulation. The overall trend for oral exposure reflected the relative trend from IV clearance, whereby the

compounds with higher IV clearance had overall lower oral AUC and $C_{max}$. Oral bioavailability was moderate in the range of 37-63% for each of the compounds with low to moderate clearance, whereas **39**, with a fairly high clearance in rat (Cl = 50.0 mL/min/kg), exhibited low oral bioavailability (%F = 4).

Compound **31** was prioritized for *in vivo* efficacy studies due to the combination of attractive *in vivo* PK properties and *in vitro* potency across all species of TRPA1 tested. Established models of somatic and visceral inflammatory pain were used according published methods.[32] The analgesic effect of **31** was evaluated in the Freund's Complete Adjuvant (FCA)-induced mechanical hyperalgesia model of inflammatory pain.[33,34] Oral administration of **31** significantly reversed intraplantar FCA-induced mechanical hyperalgesia, with 58.6% reversal after 1 h following a 10 mg/kg oral dose ($D_{50}$ = 5.5 mg/kg) (Figure 2). The effect of **31** was also evaluated in the mustard oil (MO)-induced allodynia model of visceral pain in the mouse.[35] In this model, orally administered **31** also elicited a significant reversal of MO-induced allodynia with a full effect after 1 h with a 10 mg/kg dose (Figure 3). The pharmacokinetic profile of **31** in mouse had been established to be reasonably consistent with what was observed in the rat (Table 7) with a slightly higher clearance and lower oral bioavailability.

TRP channels in general mediate thermosensation and thermoregulation in mammals, and specifically TRPA1 is believed to be a sensor of noxious cold and appears to be activated by cold temperatures. In one study, $TRPA1^{-/-}$ knockout mice displayed a reduced sensitivity to cold, as measured by paw withdrawal from a 0 °C plate or paw shaking in response to acetone-induced cooling.[17] We therefore evaluated the effect of an orally administered TRPA1 antagonist (**31**) on thermosensation in naive mice when placed upon a cold (-5 °C) surface. As shown in Figure 4, naïve mice administered with compound **31** demonstrated a reduced sensitivity to the cold

surface in a dose-dependent manner, as measured by the latency to respond with behavioural queues (determined by the time to the first observed hind paw flick/shake, lick, or jump) similar in magnitude to that observed with the TRPA1 knockout phenotype.[17]

Antagonists of the related sensory TRP channel, TRPV1, have been shown to elicit significant increases in body temperature.[36] This marked hyperthermia has limited the clinical utility of TRPV1 antagonists for the treatment of pain.[37] To understand whether TRPA1 antagonists would decrease body temperature, compound **31** was orally administered to naïve rats at and above the therapeutic dose range (Figure 5). The cannabinoid agonist WIN55,212-2[38] was chosen as the positive control because historically in our laboratory this compound induces a robust body temperature change over the course of the experiment, whereas the TRPV1 agonist capsaicin gives a shorter-duration hypothermia and could elicit a nociceptive response. Important to note for the future development potential of TRPA1 antagonists, Compound **31** did not alter body temperature despite the effect observed on noxious cold sensation.

## Conclusion

In summary, medicinal chemistry efforts initiated from a HTS hit compound **4** resulted in the discovery of a novel series of TRPA1 antagonists derived from a 5-phenyl indazole scaffold. The SAR demonstrated a strong preference for a trifluoromethyl group at the 2-position of the phenyl ring and small hydrophobic substituents at the 6-position of the indazole ring system, and in combination, provided a number of potent and selective TRPA1 antagonists. *In vivo* rodent PK of selected compounds with potent *in vitro* antagonist activities across multiple species of TRPA1 were evaluated, and they were found to have adequate pharmacokinetic profiles with modest oral bioavailability in rodents. Compound **31** was selected for further evaluation in

rodent pain models, and following a single oral dose of 10 mg/kg, compound **31** significantly reversed FCA-induced inflammatory pain in the rat as well as mustard oil-induced allodynia in the mouse. An effect on the sensation of cold at -5 °C was also observed in the mouse, which is consistent with the TRPA1 KO phenotype and TRPA1 regulation *in vitro* by noxious cold temperatures. Compound **31** and related indazoles have provided us with useful pharmacological tools in pre-clinical rodent models for the evaluation of TRPA1 as a target for the treatment of pain. Likewise, as the potential exists for the development of TRPA1 antagonists for indications beyond pain, valuable tool compounds such as **31** can be utilized in pre-clinical *in vivo* models to explore the role of TPRA1 in various disease model settings where TRPA1 is believed to play a key role.

Experimental Section

**General Methods** All commercial reagents and solvents were used as received. 5-Bromo-1*H*-indazole and *tert*-Butyl 5-(4,4,5,5-tetramethyl-1,3,2-dioxaborolan-2-yl)-1*H*-indazole-1-carboxylate were purchased from Sigma-Aldrich. 5-bromo-6-methylindazole (**6c**) was purchased from Manchester Organics. The synthetic procedures for the preparation of substituted 5-bromoindazoles **6b, 6d-j** and **7a-f** from commercial 2-methylanilines are provided in the Supporting Information. $^{1}$H and $^{13}$C NMR spectra were obtained on a Bruker AVANCE 400 NMR spectrometer using ICON-NMR. Spectra were measured at 298K and were referenced using the solvent peak. Mass spectra were run using electrospray ionization on either a Micromass Platform Mass Spectrometer or SQD Mass Spectrometer. Final compounds had a purity of ≥ 95% as assessed by analytical HPLC using either an Agilent 1100 HPLC or Waters Acquity UPLC. High resolution mass spectrometry was obtained using LTQ Orbitrap. Melting points were measured by DSC on a Perkin Elmer Pyris 1, heating from 25 °C to 300 °C at 20

°C/min under nitrogen. Elemental analysis was measured on a Leco CHNS-932. Microwave reactions were performed using a Biotage Initiator Robot Sixty. All *in vivo* study protocols were approved by the Institutional Animal Care and Use Committee (IACUC) and the Novartis Animal Welfare and Ethics Committee and performed in accordance with the National Institutes of Health Guide for the Care and Use of Laboratory Animals (USA) and Home Office (United Kingdom) guidelines.

**Typical Procedure for Suzuki Coupling of *tert*-Butyl 5-(4,4,5,5-tetramethyl-1,3,2-dioxaborolan-2-yl)-1*H*-indazole-1-carboxylate (9) used for the synthesis of 14, 15, 16, 20, 21 and 22.**

**5-(2-Isopropyl-phenyl)-1*H*-indazole (15)**

To 1-bromo-2-isopropylbenzene (43.4 mg, 0.218 mmol) in water (0.2 mL) and ethanol (0.7 mL) was added *tert*-butyl 5-(4,4,5,5-tetramethyl-1,3,2-dioxaborolan-2-yl)-1H-indazole-1-carboxylate (75 mg, 0.218 mmol), sodium carbonate (69.3 mg, 0.654 mmol) and tetrakis(triphenylphosphine)palladium(0) (50.4 mg, 0.044 mmol) and the mixture was heated to 120 ºC in the microwave for 1 h. The reaction mixture was partitioned between water and ethyl acetate. The organic layer was separated, dried over magnesium sulfate, and the solvent was evaporated. The crude residue was purified by column chromatography on silica (0-100% EtOAc/iso-hexane) to give **15** as a colorless solid (40mg, 0.169 mmol, 78% yield): $^1$H NMR (400 MHz, DMSO-$d_6$) δ 13.10 (s, 1H), 8.10 (s, 1H), 7.62 (s, 1H), 7.59 (d, $J$ = 8.5 Hz, 1H), 7.41 (d, $J$ = 7.9 Hz, 1H), 7.35 (dd, $J$ = 7.4, 7.4 Hz, 1H), 7.22 (m, 2H), 7.18 (m, 1H), 3.00 (sept, $J$ = 6.8 Hz, 1H), 1.10 (s, 6H); MS(ESI) *m/z* 237.13 $[M+H]^+$.

**Typical Procedure for Suzuki coupling of 5-Bromo-1*H*-indazole used for the synthesis of 4, 12, 17, 18, 19, 23, 24, 25, 27 and 28.**

**5-(2-(Trifluoromethyl)phenyl)-1*H*-indazole (17)**

A mixture of 5-bromo-1H-indazole (100 mg, 0.5 mmol), 2-(trifluoromethyl)phenylboronic acid (106 mg, 0.58 mmol, 1.1 equiv), $Cs_2CO_3$ (413 mg, 1.27 mmol, 2.5 equiv), chloro(di-2-norbornylphosphino)(2'-dimethylamino-1,1'-biphenyl-2-yl)palladium (II) (28 mg, 0.05 mmol, 0.1 equiv) in water (0.1 mL) and dioxane (1 mL) was sealed and heated in the microwave for 5 min at 160 ºC. The mixture was partitioned between water and EtOAc. The organic phase was separated and dried over $MgSO_4$ and then concentrated *in vacuo*. The residue was purified by silica gel chromatography to give **17** as a white solid. MP 120-126º C; $^1$H NMR (400 MHz, DMSO-$d_6$) δ 13.18 (s, 1H), 8.11 (s, 1H), 7.84 (d, $J$ = 7.9 Hz 1H), 7.72 (dd, $J$ = 7.5 Hz; 7.5 Hz, 1H), 7.68 (s, 1H), 7.61 (dd, $J$ = 7.8; 7.8 Hz, 1H), 7.59 (d, $J$ = 8.3 Hz, 1H), 7.45 (d, $J$ = 7.6 Hz, 1H), 7.28 (d, $J$ = 8.6 Hz, 1H); $^{13}$C NMR (125MHz, DMSO-$d_6$) δ 141.2 (q, $J$ = 1.8 Hz), 139.2, 133.8, 132.7, 132.1, 131.3, 127.7, 127.2, 127.0 (q, $J$ = 32 Hz), 126.0 (q, $J$ = 5.0 Hz), 124.2 (q, $J$ = 272.2 Hz), 122.4, 120.3, 109.5; $^{19}$F NMR (376 MHz, DMSO-$d_6$) δ -55.35; EA: Calc for $C_{14}H_9F_3N_2$: C, 64.12; H, 3.46; N, 10.68: Found: C, 63.99; H, 3.37, N, 10.75; HRMS *m/z* Calc for $C_{14}H_9F_3N_2$: 263.0796, Found: 263.0804.

**Typical procedure for Suzuki Coupling of 1-(5-Bromo-1*H*-indazol-1-yl)ethanones used for the synthesis of 30, 32, 33, 37, 38 and 41.**

**6-Chloro-5-(2-(trifluoromethyl)phenyl)-1*H*-indazole (30)**

A mixture of **7a** (500 mg, 2.160 mmol), 2-trifluoromethylphenylboronic acid (410 mg, 2.160 mmol), cesium carbonate (2111 mg, 6.48 mmol), tetrakis(triphenylphosphine)palladium(0) (499 mg, 0.432 mmol) in water (1 mL) and dioxane (6 mL) was sealed and heated for 1 hr at 120 ºC in the microwave. The reaction mixture was partitioned between water and ethyl acetate. The organic phase was separated, dried over magnesium sulfate, and the solvent was evaporated.

The residue was purified by silica gel chromatography (0-50% EtOAc/iso-hexane) to yield **30** as a colourless solid (70mg, 0.24 mmol, 11% yield): $^{1}$H NMR (400 MHz, DMSO-$d_6$) δ 13.35 (s, 1H), 8.14 (s, 1H), 7.86 (d, $J$ = 7.9 Hz, 1H), 7.75 (m, 3H), 7.68 (m, 1H), 7.41 (d, $J$ = 7.5 Hz, 1H); MS(ESI) *m/z* 297.19 $[M+H]^+$.

**Typical Procedure via THP Protection Route used for the synthesis of 13, 26, 31, 36, 39, 42 and 43.**

**6-Methyl-5-(2-(trifluoromethyl)phenyl)-1*H*-indazole (31)**

*5-bromo-6-methyl-1-(tetrahydro-2H-pyran-2-yl)-1H-indazole* (**8c**)

To a stirred suspension of 5-bromo-6-methyl-1H-indazole (**6c**) (10 g, 47.4 mmol) in chloroform (200 ml) was added *p*-toluenesulfonic acid monohydrate (0.901 g, 4.7 mmol) followed by 3,4-dihydro-2H-pyran (8.66 mL, 95 mmol) and the mixture was stirred at room temperature overnight. The reaction mixture was then heated at 50 °C for 5 h. The product mixture was concentrated under vacuum, dissolved in ethyl acetate, and washed with water, saturated aqueous sodium hydrogen carbonate and brine. The organics were dried over sodium sulfate, filtered and concentrated *in vacuo* to yield the title compound (15.5 g) which was used in the next step without further purification. Purification of a small sample by column chromatography (0-30% EtOAc/iso-hexane) and recrystallization from diethyl ether provided a sample for full analysis: $^{1}$H NMR (400 MHz, DMSO-$d_6$) δ 8.04 (s, 1H), 8.03 (s, 1H), 7.75 (s, 1H), 5.80 (dd, $J$ = 9.7, 2.5 Hz, 1H), 3.91-3.84 (m, 1H), 3.79-3.68 (m, 1H), 2.44 (s, 3H), 2.46-2.32 (m, 1H), 2.09-1.99 (m, 1H), 1.99-1.91 (m, 1H), 1.81-1.66 (m, 1H), 1.62-1.54 (m, 2H), $^{13}$C NMR (100 MHz, DMSO-$d_6$) δ 138.7, 134.9, 132.6, 124.0, 123.8, 117.0, 111.6, 84.0, 66.5, 28.8, 24.7, 23.4, 22.2; EA: Calc for $C_{13}H_{15}BrN_2O$: C, 52.9; H, 5.12; N, 9.49: Found: C, 53.05; H, 5.30, N, 9.51; MS(ESI) *m/z* 295.23 $[M+H]^+$.

*6-Methyl-1-(tetrahydro-2H-pyran-2-yl)-5-(2-(trifluoromethyl)phenyl)-1H-indazole* (**10c**)

A mixture of **8c** (8 g, 27.1 mmol), 2-(trifluoromethyl)phenylboronic acid (5.15 g, 27.1 mmol), cesium carbonate (26.5 g, 81 mmol), tetrakis(triphenylphosphine)palladium(0) (3.13 g, 2.71 mmol) in water (15 mL) and dioxane (80 mL) was sealed and heated in the microwave for 1 hour at 120ºC. The mixture was partitioned between water and ethyl acetate. The organic phase was separated and dried over magnesium sulfate and concentrated *in vacuo*. The residue was purified by chromatography on silica to give **10c** as a white solid (8.7 g, 24.14 mmol, 89% yield): $^{1}$H NMR (400 MHz, DMSO-$d_6$) δ 8.06 (s, 1H), 7.87 (d, $J$ = 7.9 Hz, 1H), 7.73 (dd, $J$ = 7.5; 7.5 Hz, 1H), 7.63 (m, 2H), 7.49 (s, 1H), 7.37 (dd, $J$ = 8.3, 8.3 Hz, 1H), 5.85 (m, 1H), 3.91 (m, 1H), 3.77 (m, 1H), 2.45 (m, 1H), 2.10 (s, 3H), 2.10-1.95 (m, 2H), 1.82-1.70 (m, 1H), 1.63-1.57 (m, 2H). $^{13}$C NMR (125MHz, DMSO-$d_6$) δ 140.1, 139.3, 134.6, 133.4, 132.5, 132.4, 132.4, 128.0, 127.5 (q, $J$ = 28.8 Hz), 125.8 (q, $J$ = 5.6 Hz), 124.1 (q, $J$ = 273.6Hz), 121.8, 120.8, 110.1, 83.9, 66.5, 28.9, 24.8, 22.3, 20.8; HRMS: Calc for $C_{20}H_{20}F_3N_2O$: 361.153; Found: 361.152.

*6-Methyl-5-(2-(trifluoromethyl)phenyl)-1H-indazole (**31**)*

To a solution of **10c** (5 g, 13.87 mmol) in methanol (150 mL) was added 4M HCl in dioxane (2.108 ml, 69.4 mmol) and the mixture was stirred at rt overnight then left to stand for 3 nights. The mixture was partitioned between ethyl acetate and saturated aqueous sodium hydrogen carbonate. The organic phase was separated and the aqueous extracted with ethyl acetate. The combined organics were dried over magnesium sulfate and concentrated *in vacuo*. The residue was purified by chromatography on silica (0-70% EtOAc/iso-hexane) and then was dissolved in ethanol (~100 mL) and macroporous polystyrene-2,4,6-trimercaptotriazine (4 g) was added and mixture stirred at 40°C for 1h. The mixture was filtered and to the filtrate was added a further 2 g of macroporous polystyrene-2,4,6-trimercaptotriazine and stirred 40 °C for 1 h. This was filtered

again and filtrate evaporated. The residue was recrystallized from methanol/water to give **31** as a white solid (1.52 g, 5.5 mmol, 40% yield): Mp 176-182ºC; $^{1}$H NMR (400 MHz, DMSO-$d_6$) δ 13.01 (br s, 1H), 8.00 (s, 1H), 7.85 (d, *J* = 7.7 Hz, 1H), 7.72 (m, 1H), 7.62 (m, 1H), 7.47 (s, 1H), 7.43 (s, 1H), 7.35 (d, *J* = 7.5 Hz, 1H), 2.05 (s, 3H); $^{13}$C NMR (125MHz, DMSO-$d_6$) δ 140.4 (q, *J* = 2.1 Hz), 139.9, 134.1, 133.4, 132.4, 132.1, 131.6, 127.9, 127.6 (q, *J* = 28.5 Hz), 125.9 (q, *J* = 5.4 Hz), 124.1 (q, *J* = 274.9 Hz), 120.7, 120.4, 109.8, 20.7; $^{19}$F NMR (400 MHz, DMSO-$d_6$) δ -57.48; EA: Calc for $C_{15}H_{11}F_3N_2$: C, 65.22; H, 4.01; N, 10.14: Found: C, 65.04; H, 4.32, N, 10.28; MS(ESI) *m/z* 277.16 $[M+H]^+$.

**1-Methyl-5-(2-(trifluoromethyl)phenyl)-1*H*-indazole (29)**

**17** (80 mg; 0.3 mmol) was added to a mixture of 60 % NaH (15 mg; 0.37 mmol) in DMF (1 mL). After 15 min at room temperature, iodomethane (52 mg; 0.36 mmol) was added, the reaction was stirred for 2 hr, and then diluted with water and extracted with EtOAc. The extracts were rinsed with water and brine, dried over magnesium sulfate evaporated, and the product **29** isolated by HPLC: $^{1}$H NMR (400 MHz, DMSO-$d_6$) δ 8.10 (s, 1H), 7.83 (d, *J* = 7.8 Hz, 1H), 7.75-7.62 (m, 3H), 7.61 (dd, *J* = 7.6, 7.6 Hz, 1H), 7.44 (d, *J* = 7.6 Hz, 1H), 7.32 (d, *J* = 8.9 Hz, 1H), 4.10 (s, 3H).MS(ESI) m/z 277.1 $[M+H]^+$.

**6-Cyclopropyl-5-(2-(trifluoromethyl)phenyl)-1*H*-indazole (34)**

*1-(Tetrahydro-2H-pyran-2-yl)-5-(2-(trifluoromethyl)phenyl)-1H-indazol-6-ol* (**50**)

To a solution of 1-dodecanethiol (1.613 g, 7.97 mmol) in anhydrous N-methyl-2-pyrrolidinone (3 ml) under nitrogen was added sodium hydroxide (638 mg, 15.94 mmol). The resulting mixture was stirred at room temperature for 30 minutes and treated with **10d** (2.0 g, 5.31 mmol) in N-methyl-2-pyrrolidinone (7 mL) via syringe. The vial was subsequently sealed and heated at 130 °C. After 5 h, the mixture was acidified with 2M hydrochloric acid and extracted with ethyl

acetate. The combined organic extracts were dried over magnesium sulfate, filtered and concentrated to give a yellow oil. The residue was purified by chromatography on silica (0-100% EtOAc/iso-hexane) to afford **50** as a foamy colorless solid (1.84 g, 5.08 mmol, 96% yield): $^1$H NMR (400 MHz, DMSO-$d_6$) δ 9.80 (s, 1H), 7.95 (s, 1H), 7.80 (d, $J$ = 7.9 Hz, 1H), 7.70 (dd, $J$ = 7.5, 7.5 Hz, 1H), 7.60 (dd, $J$ = 7.7, 7.7 Hz, 1H), 7.40 (s, 1H), 7.35 (dd, $J$ = 7.7, 7.7 Hz, 1H), 7.0 (s, 1H), 5.70 (m, 1H), 3.90 (m, 1H), 3.70 (m, 1H), 2.40 (m, 1H), 2.05 (m, 2H), 1.75 (m, 1H), 1.60 (m, 2H); MS(ESI) *m/z* 363.3 $[M+H]^+$.

*1-(Tetrahydro-2H-pyran-2-yl)-5-(2-(trifluoromethyl)phenyl)-1H-indazol-6-yl trifluoromethanesulphonate (**51**)*

1-(Tetrahydro-2H-pyran-2-yl)-5-(2-(trifluoromethyl)phenyl)-1H-indazol-6-ol (**50**) (100 mg, 0.276 mmol), phenyl triflimide (99 mg, 0.276 mmol) and potassium carbonate (114 mg, 0.828 mmol) in tetrahydrofuran (1 mL) were heated using microwave radiation at 120 °C for 24 minutes. After cooling, the mixture was filtered and washed with ethyl acetate. The filtrate was evaporated to give a pink residue. The residue was purified by chromatography on silica (0-100% EtOAc/iso-hexane) followed by repurification (0-30% EtOAc/iso-hexane) to afford **51** (110 mg, 0.21 mmol, 77% yield): $^1$H NMR (400 MHz, $CDCl_3$) δ 8.02 (s, 1H), 7.72 (d, $J$ = 7.9 Hz, 1H), 7.64 (s, 1H), 7.58 (d, $J$ = 5.8 Hz, 1H), 7.51 (m, 2H), 7.31 (m, 1H), 5.69 (m, 1H), 3.98 (m, 1H), 3.72 (m, 1H), 2.48 (m, 1H), 2.10 (m, 2H), 1.70 (m, 3H); 19F (376 MHz, $CDCl_3$) δ -59, -74; MS(ESI) *m/z* 495.4 $[M+H]^+$.

*6-Cyclopropyl-1-(tetrahydro-2H-pyran-2-yl)-5-(2-(trifluoromethyl)phenyl)-1H-indazole* (**52**)

1-(Tetrahydro-2H-pyran-2-yl)-5-(2-(trifluoromethyl)phenyl)-1H-indazol-6-yl trifluoromethanesulphonate (**51**) (110 mg, 0.222 mmol), cyclopropylboronic acid (287 mg, 3.34 mmol), tetrakis(triphenylphosphine)palladium(0) (51 mg, 0.044 mmol) and cesium carbonate

(217 mg, 0.667 mmol) in dioxane (2 mL) and water (0.22 mL) were heated using microwave radiation at 100 °C for 1 h. After cooling to room temperature, the reaction was quenched with water and extracted with ethyl acetate. The combined organic extracts were dried over magnesium sulfate, filtered and concentrated *in vacuo* to give a yellow residue. The residue was purified by chromatography on silica (0-60% EtOAc/iso-hexane) to afford **52** (63mg, 0.15 mmol, 68% yield): MS(ESI) *m/z* 387.4 $[M+H]^+$.

*6-Cyclopropyl-5-(2-(trifluoromethyl)phenyl)-1H-indazole* (**34**)

To a solution of **52** (63 mg, 0.163 mmol) in methanol (1 mL) was added 4M hydrogen chloride in dioxane (0.204 mL, 0.815 mmol). The reaction mixture was stirred at room temperature overnight. The solvent was removed *in vacuo,* and the residue was diluted with ethyl acetate and basified with saturated aqueous sodium hydrogen carbonate. The combined organic extracts were dried over magnesium sulfate, filtered and concentrated *in vacuo*. The residue was purified by chromatography on silica (0-100% EtOAc/iso-hexane) to afford an oily residue. The residue was recrystallized from 1:1 methanol/water, passed through an Isolute® PE-AX cartridge rinsing with methanol before the product was eluted with ammonia in methanol. This afforded **34** as a colorless solid (18.6 mg, 0.062 mmol, 38% yield): $^1$H NMR (400 MHz, $CDCl_3$) δ 8.10 (s, 1H), 7.81 (d, *J* = 7.9 Hz, 1H), 7.60 (dd, *J* = 7.2, 7.2 Hz, 1H), 7.56-7.50 (m, 2H), 7.39 (d, *J* = 7.5 Hz, 1H), 7.14 (s, 1H), 1.51-1.60 (m, 1H), 0.73-0.86 (m, 3H), 0.59-0.67 (m, 1H); $^{19}$F (376 MHz, $CDCl_3$) δ -58.2; MS(ESI) *m/z* 303.3 $[M+H]^+$.

**6-(Difluoromethyl)-5-(2-(trifluoromethyl)phenyl)-1*H*-indazole (35)**

*Methyl 1-(tetrahydro-2H-pyran-2-yl)-5-(2-(trifluoromethyl) phenyl)-1H-indazole-6-carboxylate* (**10h**)

**10h** was prepared analogously to **10c**: $^1$H NMR (400 MHz, DMSO-$d_6$) δ 8.36 (d, $J$ = 3.6 Hz, 1H), 8.25 (s, 1H), 7.78 (d, $J$ = 8.4 Hz, 1H), 7.68 (s, 1H), 7.66 (d, $J$ = 7.5 Hz, 1H), 7.59 (dd, $J$ = 7.6, 7.6 Hz, 1H), 7.32 (dd, $J$ = 7.0, 7.0 Hz, 1H), 6.09-6.04 (m, 1H), 3.90-3.78 (m, 2H), 2.48-2.38 (m, 1H), 2.10-2.00 (m, 2H), 1.83-1.74 (m, 1H), 1.64-1.57 (m, 2H); MS(ESI) *m/z* 306.15 $[M+H]^+$.

*(1-(Tetrahydro-2H-pyran-2-yl)-5-(2-(trifluoromethyl)phenyl)-1H-indazol-6-yl)methanol* (**45**)

To an ice cooled solution of **10h** (968 mg, 2.394 mmol) in tetrahydrofuran (5 mL) under nitrogen was added lithium aluminum hydride (2M in THF) (4.79 ml, 9.58 mmol). The mixture was stirred with ice cooling for 30 minutes and then allowed to warm to room temperature over 1.5 h. To the mixture was added water (360 µL), followed by 2M sodium hydroxide (360 µL), water (1 mL) and 2M sodium hydroxide (1 mL). The quenched mixture was left at room temperature overnight. The resulting suspension filtered and washed with dichloromethane. The filtrate was diluted with water and the organic portion was separated, washed with water, dried over sodium sulfate and concentrated *in vacuo*. The residue was purified by chromatography on silica (0-100% EtOAc/iso-hexane) to afford **45** as a white solid (622mg, 1.65 mmol, 69% yield): $^1$H NMR (400 MHz, DMSO-$d_6$) δ 8.08 (s, 1H), 7.85 (m, 2H), 7.71 (dd, $J$ = 7.5, 7.5 Hz, 1H), 7.63 (dd, $J$ = 7.6, 7.6 Hz, 1H), 7.47 (s, 1H), 7.38 (dd, $J$ = 8.1, 8.1 Hz, 1H), 5.92-5.87 (m, 1H), 5.30 (t, $J$ = 5.2 Hz, 1H), 4.27 (m, 1H), 4.15 (m, 1H), 3.96-3.87 (m, 1H), 3.82-3.73 (m, 1H), 2.49-2.40 (m, 1H), 2.10-1.97 (m, 2H), 1.86-1.74 (m, 1H), 1.60 (m, 2H): MS(ESI) *m/z* 377.35 $[M+H]^+$.

*1-(Tetrahydro-2H-pyran-2-yl)-5-(2-(trifluoromethyl)phenyl)-1H-indazole-6-carbaldehyde* (**46**)

To a solution of **45** (250 mg, 0.664 mmol) in dichloromethane (10 mL) was added manganese dioxide (289 mg, 3.32 mmol) and the mixture was stirred at room temperature for 3 days. The resulting mixture was filtered through Celite® and washed with dichloromethane. The filtrate was concentrated *in vacuo* and purification of the residue by chromatography on silica (0-50%

EtOAc/iso-hexane) afforded **46** (153mg, 0.41 mmol, 62% yield): $^1$H NMR (400 MHz, DMSO-$d_6$) δ 9.76 (s, 1H), 8.39 (d, *J* = 6.2 Hz, 1H), 8.29 (s, 1H), 7.87 (d, *J* = 7.8 Hz, 1H), 7.75 (s, 1H), 7.73 (d, *J* = 7.4 Hz, 1H), 7.67 (dd, *J* = 7.7, 7.7 Hz, 1H), 7.45 (dd, *J* = 7.5, 7.5 Hz, 1H), 6.11-6.06 (m, 1H), 3.97-3.78 (m, 2H), 2.48-2.39 (m, 1H), 2.10-2.02 (m, 2H), 1.86-1.73 (m, 1H), 1.65-1.57 (m, 2H); MS(ESI) *m/z* 291.30 $[M+H]^+$.

*6-(Difluoromethyl)-1-(tetrahydro-2H-pyran-2-yl)-5-(2-(trifluoromethyl)phenyl)-1H-indazole* (**48**)

**46** (25mg, 0.067 mmol) was dissolved in dry dichloromethane (1 mL) and to this was added diethylaminosulfur trifluoride (13µl, 0.10 mmol, 1.5 equiv) and the reaction was heated to reflux overnight. Additional diethylaminosulfur trifluoride (25µl, 0.2 mmol) was added and the mixture was heated to reflux overnight. The reaction mixture cooled, diluted with dichloromethane and washed with saturated aqueous sodium carbonate, 1M hydrochloric acid and brine. The organic phase was dried over magnesium sulfate and solvent removed *in vacuo*. The residue was purified by column chromatography (10% EtOAc/iso-hexane) to yield **49** (12 mg, 0.030 mmol, 45% yield): $^1$H NMR (400MHz, $CDCl_3$) δ 8.00 (s, 1H), 7.91 (s, 1H), 7.70 (d, *J* = 7.5 Hz, 1H), 7.50 (m, 3H), 7.25 (m, 1H), 6.29 (t, *J* = 55.3 Hz, 1H), 5.75 (d, *J* = 9.3 Hz, 1H), 4.01 (m, 1H), 3.72 (m, 1H), 2.55 (m, 1H), 2.09 (m, 2H), 1.69 (m, 3H); MS(ESI) *m/z* 313.2 $[MH-THP]^+$.

*6-(Difluoromethyl)-5-(2-(trifluoromethyl)phenyl)-1H-indazole* (**35)**

**49** (12mg, 0.03 mmol) was dissolved in dioxane (100 µL) and to this was added 4M hydrogen chloride in dioxane (40 µL, 0.151 mmol) and methanol (100 µL). This was left to stir for 4 hours at room temperature, then heated to 50°C overnight. The reaction mixture was concentrated *in vacuo* to yield **35** (3 mg, 0.0096 mmol, 37% yield): $^1$H NMR (400MHz, $CDCl_3$) δ 8.05 (s, 1H),

7.81 (s, 1H), 7.70 (d, *J* = 7.5 Hz, 1H), 7.55 (s, 1H), 7.48 (m, 2H), 7.25 (d, *J* = 7.3 Hz, 1H), 6.25 (t, *J* = 55.4 Hz, 1H); MS(ESI) *m/z* 313.1 $[M+H]^+$.

**6-(Methoxymethyl)-5-(2-(trifluoromethyl)phenyl)-1*H*-indazole (40)***6-(Methoxymethyl)-1-(tetrahydro-2H-pyran-2-yl)-5-(2-(trifluoromethyl)phenyl)-1H-indazole* (**48**)

To a slurry of sodium hydride (60% in mineral oil) (12.75 mg, 0.319 mmol) in N,N-dimethylformamide (2.5 ml) cooled in an ice-bath was added a solution of **45** (100 mg, 0.266 mmol) in N,N-dimethylformamide (1.5 mL) and the mixture was stirred at 0°C. After 1 h, methyl iodide (0.020 ml, 0.319 mmol) was added to the mixture and it was allowed to warm to room temperature and stirred for 1.5 h. The mixture was added to ice water, and a white precipitate formed which was removed by filtration. The filtrate was extracted with ethyl acetate. The organic extracts were washed with water, dried over magnesium sulfate, filtered and concentrated *in vacuo* to give **48** as an oil (97 mg, 0.25 mmol, 94% yield): $^1$H NMR (400 MHz, $CDCl_3$) δ 8.04 (s, 1H), 7.79 (d, *J* = 7.8 Hz, 1H), 7.76 (s, 1H), 7.58 (m, 1H), 7.54 (m, 1H), 7.52 (s, 1H), 7.30 (m, 1H), 5.80 (d, *J* = 9.6 Hz, 1H), 4.27-4.18 (m, 1H), 4.14 (m, 1H), 3.82 (m, 1H), 3.32 (s, 3H), 2.70-2.59 (m, 1H), 2.24-2.07 (m, 1H), 1.88-1.60 (m, 1H), 1.72-1.58 (m, 1H), 1.28 (s, 2H), 0.94-0.85 (m, 1H); MS(ESI) *m/z* 391.37 $[M+H]^+$.

*6-(Methoxymethyl)-5-(2-(trifluoromethyl)phenyl)-1H-indazole* (**40)**

To a solution of **48** (97 mg, 0.248 mmol) in dioxane (0.5 mL) was added 4M hydrogen chloride in dioxane (0.311 mL, 1.242 mmol) followed by methanol (2 mL) and the mixture was stirred at room temperature overnight. The reaction mixture was diluted in ethyl acetate and washed with water, saturated aqueous sodium hydrogen carbonate and brine. The organic extracts were dried over sodium sulfate, filtered and concentrated under vacuum. The crude residue was purified by column chromatography on silica (0-100% EtOAc/iso-hexane) to give **40** as a white glassy solid

(57.7 mg, 0.19 mmol, 76% yield): $^1$H NMR (400 MHz, $CDCl_3$) δ 8.10 (s, 1H), 7.80 (d, *J* = 7.7 Hz, 1H), 7.70 (s, 1H), 7.59 (m, 1H), 7.57 (s, 1H), 7.53 (m, 1H), 7.34 (d, *J* = 7.4 Hz, 1H), 4.22 (s, 1H), 3.32 (s, 3H); MS(ESI) *m/z* 307.29 $[M+H]^+$.

**5-(2-Trifluoromethyl-phenyl)-1*H*-indazole-6-carboxylic acid methylamide (44)**

*1-(tetrahydro-2H-pyran-2-yl)-5-(2-(trifluoromethyl)phenyl)-1H-indazole-6-carboxylic acid* (**47**)

To a solution of **10h** (889 mg, 2.198 mmol) in tetrahydrofuran (10 mL) was added sodium hydroxide (879 mg, 21.98 mmol), water (1.67 mL) and methanol (10 mL), and this was stirred at room temperature overnight. The reaction mixture was concentrated under vacuum and 2M hydrochloric acid was added until the reaction mixture was pH 2. This was extracted with ethyl acetate and the organic extracts washed with saturated aqueous sodium hydrogen carbonate and brine, dried over sodium sulfate, and concentrated *in vacuo*. The product **47** was used in the following step without further purification (984 mg): $^1$H NMR (400 MHz, DMSO-$d_6$) δ 12.5 (s, 1H), 8.35 (d, 1H), 8.22 (s, 1H), 7.76 (d, *J* = 7.7 Hz, 1H), 7.64-7.60 (m, 2H), 7.56 (dd, *J* = 7.5, 7.5 Hz, 1H), 7.361 (dd, *J* = 6.2, 6.2 Hz, 1H), 6.07-6.00 (m, 1H), 3.96-3.76 (m, 2H), 2.48-2.37 (m, 1H), 2.10-1.98 (m, 2H), 1.86-1.74 (m, 1H), 1.64-1.57 (m, 2H); MS(ESI) *m/z* 391.43 $[M+H]^+$.

*5-(2-Trifluoromethyl-phenyl)-1H-indazole-6-carboxylic acid methylamide* (**44**)

To a solution of **47** (75 mg, 0.192 mmol) in toluene (0.5 mL) was added thionyl chloride (0.5 mL, 6.85 mmol) and the mixture was heated at 70 °C for 4 h after which time the thionyl chloride was removed under vacuum. The residue was dissolved in toluene (0.5 mL) and diisopropylethylamine (0.2 mL, 1.153 mmol) and methylamine (2M in tetrahydrofuran) (0.38 mL, 0.769 mmol) were added and the mixture was stirred at 70 °C overnight. Water was added and the mixture was extracted with dichloromethane. The organic extracts were washed with saturated aqueous sodium hydrogen carbonate, dried over sodium sulfate and concentrated *in*

*vacuo*. The residue was purified by preparative reverse phase HPLC (40-80% $CH_3CN$/water with 0.1% TFA) to yield **44** as a white glassy solid (13.4 mg, 0.042 mmol, 21.8% yield): $^1$H NMR (400 MHz, DMSO-$d_6$) δ 13.4 (s, 1H), 8.24 (m, 1H), 8.13 (s, 1H), 7.73 (d, $J$ = 7.7 Hz, 1H), 7.69 (s, 1H), 7.60 (dd, $J$ = 7.4; 7.4 Hz, 1H), 7.56 (s, 1H), 7.52 (m, 1H), 7.30 (d, $J$ = 7.5 Hz, 1H), 2.57 (d, $J$ = 4.6 Hz, 3H); MS(ESI) *m/z* 320.30 $[M+H]^+$.

**TRP channel cellular assays**

Full length human, rat, or mouse TRPA1 cDNA was sub-cloned into the expression vector pcDNA™4/TO/myc-His (Invitrogen) and stable expression clones were created in CHO-TREX cells. Stable human TRPV1 and TRPM8-expressing clones were similarly created in CHO-K1 using the plasmids pcDNA™3.1 (Geneticin) and pcDNA™3.1 (Hygromycin) respectively. Human TRPV3 expression clones were created in CHO-K1 cells using the vector pcDNA™3.1 (Hygromycin).

Human TRPA1 cells were maintained in Hams F-12 nutrient mixture (HyClone) containing 10% Fetal Bovine Serum (FBS, Invitrogen), 5 µg/mL Blasticidin (Invitrogen), 200 µg/mL Hygromycin B (Invitrogen), 1% antibiotic/antimycotic solution (Invitrogen), and 1% sodium pyruvate (Invitrogen). CHO-TREX cells stably expressing mouse and rat TRPA1 (CHO-mTRPA1 and CHO-rTRPA1) were maintained in Ham's F12 nutrient mix, 10% FBS, 1% antibiotics/antimycotics, 5 µg/mL blasticidin, 300 µg/mL Zeocin (Invitrogen). For compound screening, a similar medium was used containing 0.5 µg/mL or 1 µg/mL of tetracycline (Sigma) for human TRPA1, or mouse or rat TRPA1 cells, respectively. TRPV1 cell lines were grown in MEM Alpha, 10% FBS, 1% antibiotic/antimycotic solution, and 500 µg/mL G418 (Invitrogen). TRPV3 cells were grown in Ham's F12 with 10% FBS, 1% antibiotic/antimycotic, and 300

μg/mL hygromycin. TRPM8 cells were grown in DMEM with 10% FBS, 1% antibiotic/antimycotic, and 300 μg/mL hygromycin.

Compounds were serially-diluted in DMSO and stock solutions were then made in assay buffer containing HBSS and 20 mM HEPES (Gibco), 2.5 mM probenecid (Sigma), and 0.1% BSA. Cells were incubated with the calcium indicator dye Fluo4-AM (Molecular Probes) at [1ug/ml concentration] for 90 min at room temperature, washed once with assay buffer, then transferred to the FLIPR (Molecular Devices) in assay buffer for calcium flux imaging. Antagonist compounds were added to the cells first, followed 10 min later by addition of the agonists cinnamaldehyde (Sigma Aldrich), AITC (Fluka), 2-Aminoethoxydiphenylborane (2-APB, Tocris Bioscience), or dibenzo[b,f][1,4]oxazepine-4-carboxamide, which was synthesized according to the literature procedures.[23]

Agonists are used at $EC_{80}$ concentration for the respective assay:

CHO-hTRPA1: 30 μM cinnamaldehyde

CHO-hTRPA1: 2.5 μM allyl isothiocyanate (AITC)

CHO-hTRPA1: 5 nM dibenzo[b,f][1,4]oxazepine-4-carboxamide

CHO-rTRPA1: 40 μM cinnamaldehyde

CHO-mTRPA1: 40 μM cinnamaldehyde

CHO-hTRPV1: 40 nM capsaicin

CHO-hTRPV3: 40 μM 2-Aminoethoxydiphenylborane (2-APB)

CHO-hTRPM8: 40 μM menthol

Data was exported using the FLIPR software, applying the bias subtraction and the spatial uniformity, and calculated as the stop response (the time point when the positive control gave

maximal response minus the minimum response. The mean of triplicate values were used to calculate the inhibition and to plot sigmoidal dose response curves. Dose response curves were fitted using an XLfit program to determine $IC_{50}$ values.

**Freund's complete adjuvant induced mechanical hyperalgesia.**

Male wistar rats (200-250g) were used for the study. Mechanical hyperalgesia was assessed by measuring ipsi and contralateral hindpaw withdrawal thresholds to a pressure stimulus applied by an analgesymeter (Ugo Basile, Italy) with a cut off threshold of 180 g. The endpoint was taken as the first sign of pain response (struggling, vocalization, or paw withdrawal). Withdrawal thresholds of both hind paws were measured immediately before and 72 h after intraplantar injection of 25 ml of complete Freund's adjuvant (CFA) into one hind paw, and at 1,3,6h after oral administration of vehicle (0.5% methylcellulose and 0.5%Tween 80) or compound **31** (3, 10 or 30 mg/kg). $D_{50}$ refers to the calculated dose at which 50% reversal of mechanical hyperalgesia would be observed.

Reversal of established hyperalgesia was calculated according to the formula:

% Reversal

$$\frac{\text{Postdose threshold - Predose threshold}}{\text{Naive threshold - Predose threshold}} \times 100$$

**Mustard oil-Induced Allodynia Model.** C57Bl6 male mice (20-25g) were anesthetized with isoflurane and mustard oil (0.25% in 70% ethanol; 50 ml per mouse) was administered by inserting a fine cannula with a rounded tip (3 cm long) into the colon via the anus. Referred allodynia was measured from withdrawal thresholds to the application of von Frey

filaments(Semmes-Weinsten Monofilaments; Linton Instrumentation,UK) to the abdomen of mice before (baseline) and 48 h after administration of mustard oil. Animals were placed in a raised Perspex ventilated box with a wire mesh floor and allowed to acclimatize prior to measurement of withdrawal thresholds. Allodynia was tested by touching the lower abdomen with von Frey filaments in ascending order of force (0.02–15 g) for up to 6 s. The endpoint (response) was taken as an abdominal retraction, jumping, or immediate licking or scratching of the site of filament application and the lowest force required to elicit a response was recorded as withdrawal threshold (in grams). Vehicle (0.5% methylcellulose and 0.5% tween 80) and compound **31** (3, 10 and 30mg/kg) were administered orally 48h after mustard oil and referred allodynia measured 1h later.

**Thermosensation** A clear Plexiglas chamber containing a Peltier-cooled cold plate, temperature controller, and heat sink (TECA) was used to assess cold responses. Mice were weighed and treated via oral gavage with vehicle (0.5% methylcellulose and 0.5% Tween80) or compound **31** (10mg/kg or 100mg/kg) (n = 7 mice per group) and acclimated in an equivalent chamber at room temperature for 40 min. Individual mice were placed on -5 °C cold plate and observed for up to 2 min . Latency to onset was then assessed by counting the first jump, brisk hindpaw lift or flicking/licking of the hindpaws.

**Body Temperature Measurement.** Rectal temperatures in rats were measured by using a rectal probe before and 1, 3, and 6 h after oral administration of vehicle (0.5%methylcellulose and 0.5%Tween 80), compound **31** (10, 30 and 100 mg/kg p.o.) or WIN55,212-2 (6mg/kg s.c).

ACKNOWLEDGMENT. The authors thank the Analytical Chemistry and Metabolism and Pharmacokinetics groups for their contributions.

SUPPORTING INFORMATION

General procedures and experimental details for the syntheses of key intermediates used for the preparation of compounds **11-44**, and analytical data for final compounds. This material is available free of charge via the Internet at http://pubs.acs.org.

Corresponding Author E-mail: david.tully@novartis.com; Current Address: Novartis Institutes for Biomedical Research, 4560 Horton St, Emeryville, California 94608.

Ancillary Information

Abbreviations and acronyms used: DAST (Diethylaminosulfur trifluoride), FLIPR® (Fluorometric Imaging Plate Reader, Molecular Devices), HBSS (Hank's Balanced Salt Solution), HEPES (4-(2-hydroxyethyl)-1-piperazineethanesulfonic acid), AITC (allyl isothiocyanate)

REFERENCES

(1) Du, S.; Araki, I.; Kobayashi, H.; Zakoji, H.; Sawada, N.; Takeda, M. Differential expression profile of cold (TRPA1) and cool (TRPM8) receptors in human urogenital organs. *Urology* **2008**, *72*, 450-455.

(2) Nozawa, K.; Kawabata-Shoda, E.; Doihara, H.; Kojima, R.; Okada, H.; Mochizuki, S.; Sano, Y.; Inamura, K.; Matsushime, H.; Koizumi, T.; Yokoyama, T.; Ito, H. TRPA1 regulates gastrointestinal motility through serotonin release from enterochromaffin cells. *Proc. Natl. Acad. Sci. USA* **2009**, *106*, 3408-3413.

(3) Story, G. M.; Peier, A. M.; Reeve, A. J.; Eid, S. R.; Mosbacher, J.; Hricik, T. R.; Earley, T. J.; Hergarden, A. C.; Andersson, D. A.; Hwang, S. W.; McIntyre, P.; Jegla, T.; Bevan, S.;

Patapoutian, A. ANKTM1, a TRP-like channel expressed in nociceptive neurons, is activated by cold temperatures. *Cell* **2003**, *112*, 819-829.

(4) Weinhold, P.; Gratzke, C.; Streng, T.; Stief, C.; Andersson, K. E.; Hedlund P. TRPA1 receptor induced relaxation of the human urethra involves TRPV1 and cannabinoid receptor mediated signals, and cyclooxygenase activation. *J. Urol.* **2010**, *183*, 2070-2076.

(5) Doerner, J. F.; Gisselmann, G.; Hatt, H.; Wetzel, C. H. Transient Receptor Potential Channel A1 is directly gated by calcium ions *J. Biol. Chem.* **2007**, *282*, 13180-13189.

(6) Wang, Y. Y; Chang, R. B.; Waters, H. N.; McKemy, D. D.; Liman, E. R. The nociceptor ion channel TRPA1 is potentiated and inactivated by permeating calcium ions *J. Biol. Chem.* **2008**, *283*, 32691-32703.

(7) Trevisani, M.; Siemens, J.; Materazzi, S.; Bautista, D. M.; Nassini, R.; Campi, B.; Imamachi, N.; Andre, E.; Patacchini, R.; Cottrell, G. S.; Gatti, R.; Basbaum, A. I.; Bunnett, N. W.; Julius, D.; Geppetti, P. 4-Hydroxynonenal, an endogenous aldehyde, causes pain and neurogenic inflammation through activation of the irritant receptor TRPA1. *Proc. Natl. Acad. Sci. USA* **2007**, *104*, 13519–13524.

(8) Bautista, D. M.; Jordt, S. E.; Nikai, T.; Tsuruda, P. R.; Read, A. J.; Poblete J.; Yamoah, E.N.; Basbaum, A. I.; Julius, D. TRPA1 mediates the inflammatory actions of environmental irritants and proalgesic agents. *Cell* **2006**, *124*, 1269-1282.

(9) Macpherson, L. J.; Dubin, A. E.; Evans, M. J.; Marr, F.; Schultz, P. G.; Cravatt, B. F.; Patapoutian, A. Noxious compounds activate TRPA1 ion channels through covalent modification of cysteines. *Nature* **2007**, *445*, 541-545

(10) Engel, M. A.; Leffler, A.; Niedermirtl, F.; Babes, A.; Zimmermann, K.; Filipović, M. R.; Izydorczyk, I.; Eberhardt, M.; Kichko, T. I.; Mueller-Tribbensee, S. M.; Khalil, M.; Siklosi, N.; Nau, C.; Ivanović-Burmazović, I.; Neuhuber, W. L.; Becker, C.; Neurath, M. F.; Reeh, P. W. TRPA1 and substance P mediate colitis in mice. *Gastroenterology* **2011**, *141*, 1346-1358.

(11) Kunkler, P. E.; Ballard, C. J.; Oxford, G. S.; Hurley, J. H. TRPA1 receptors mediate environmental irritant-induced meningeal vasodilatation. *Pain* **2011**, *152*, 38-44.

(12) Andrade, E. L.; Forner, S.; Bento, A.; Leite, D. F. P.; Dias, M. A.; Leal, P. C.; Koepp, J.; Calixto, J. B. TRPA1 receptor modulation attenuates bladder overactivity induced by spinal cord injury. *Am. J. Physiol. Renal. Physiol.* **2011,** *300*, F1223–F1234.

(13) Kremeyer, B.; Lopera, F.; Cox, J. J.; Momin, A.; Rugiero, F.; Marsh, S.; Woods, C. G.; Jones, N. G.; Paterson, K. J.; Fricker, F. R.; Villegas, A.; Acosta, N.; Pineda-Trujillo, N. G.; Ramírez, J. D.; Zea, J.; Burley, M. W.; Bedoya, G.; Bennett, D. L.; Wood, J. N.; Ruiz-Linares, A. A gain-of-function mutation in TRPA1 causes familial episodic pain syndrome. *Neuron* **2010**, *66*, 671-680.

(14) Andersson, D. A.; Gentry, C.; Moss, S.; Bevan, S. Transient receptor potential A1 is a sensory receptor for multiple products of oxidative stress. *J. Neurosci.* **2008**, *8*, 2485-2494.

(15) Taylor-Clark, T. E.; McAlexander, M. A.; Nassenstein, C.; Sheardown, S. A.; Wilson, S.; Thornton, J.; Carr, M. J.; Undem, B. J. Relative contributions of TRPA1 and TRPV1 channels in the activation of vagal bronchopulmonary C-fibres by the endogenous autacoid 4-oxononenal. *J. Physiol* **2008**, *86*, 3447-3459**.**

(16) Yu, S.; Gao, G.; Peterson, B. Z.; Ouyang, A. TRPA1 in mast cell activation-induced long-lasting mechanical hypersensitivity of vagal afferent C-fibers in guinea pig esophagus. *Am. J. Physiol. Gastrointest. Liver Physiol.* **2009**, *297*, G34-G42.

(17) Kwan, K. Y.; Allchorne, A. J.; Vollrath, M. A.; Christensen, A. P.; Zhang, D. S.; Woolf, C. J.; Corey, D. P. TRPA1 contributes to cold, mechanical, and chemical nociception but is not essential for hair-cell transduction. *Neuron* **2006**, *50*, 277-289.

(18) Salat, K.; Moniczewski, A.; Librowski, T. Transient receptor potential channels - emerging novel drug targets for the treatment of pain. *Curr. Med. Chem*. **2013**, *20*, 1409-1436.

(19) Brederson, J.-D.; Kym, P. R.; Szallasi, A. Targeting TRP channels for pain relief. *Eur. J. Pharmacol.* **2013**, *716*, 61-76.

(20) Baraldi, P.; Preti, D.; Materazzi, S.; Geppetti, P. Transient receptor potential ankyrin 1 (TRPA1) channel as emerging target for novel analgesics and anti-inflammatory agents *J. Med. Chem.* **2010,** *53*, 5085-5107.

(21) Petrus, M.; Peier, A. M.; Bandell, M.; Hwang, S. W.; Huynh, T.; Olney, N.; Jegla, T.; Patapoutian, A. A role of TRPA1 in mechanical hyperalgesia is revealed by pharmacological inhibition. *Mol. Pain* **2007**, *3*, 40.

(22) McGaraughty, S.; Chu, K. L.; Perner, R. J.; Didomenico, S.; Kort, M. E.; Kym, P. R. (2010) TRPA1 modulation of spontaneous and mechanically evoked firing of spinal neurons in uninjured, osteoarthritic, and inflamed rats. *Mol. Pain* **2010**, *6*, 14.

(23) Chen, J.; Joshi, S. K.; DiDomenico, S.; Perner, R. J.; Mikusa, J. P.; Gauvin, D. M.; Segreti, J. A.; Han, P.; Zhang, X. F.; Niforatos W, Bianchi BR, Baker SJ, Zhong C, Simler GH,

McDonald HA, Schmidt RG, McGaraughty SP, Chu KL, Faltynek CR, Kort ME, Reilly RM, Kym PR. Selective blockade of TRPA1 channel attenuates pathological pain without altering noxious cold sensation or body temperature regulation. *Pain* **2011**, *152*, 1165-1172.

(24) Eid, S. R.; Crown, E. D.; Moore, E. L.; Liang, H. A.; Choong, K. C.; Dima, S.; Henze, D. A.; Kane, S. A.; Urban MO. HC-030031, a TRPA1 selective antagonist, attenuates inflammatory- and neuropathy-induced mechanical hypersensitivity. *Mol. Pain* **2008**, *4*, 48.

(25) Wei, H.; Hämäläinen, M. M.; Saarnilehto, M.; Koivisto, A.; Pertovaara, A. Attenuation of mechanical hypersensitivity by an antagonist of the TRPA1 ion channel in diabetic animals. *Anesthesiology* **2009**, *111*, 147-154.

(26) Chen, J.; McGaraughty, S.; Kym, P. TRPA1 in drug discovery. *TRP Channels in Drug Discovery* **2012**, *1*, 43-59.

(27) De Petrocellis, L.; Schiano Moriello, A. 2-Amino-4-arylthiazole compounds as TRPA1 antagonists (WO 2012085662): a patent evaluation. *Expert Opin. Ther. Patents* **2013**, *23*, 119-147.

(28) Düfert, M. A.; Billingsley, K.L.; Buchwald, S.L. Suzuki-Miyaura cross-coupling of unprotected, nitrogen-rich heterocycles: substrate scope and mechanistic investigation *J. Am. Chem. Soc.* **2013**, *135*, 12877-12885.

(29) Gijsen, H J. M.; Berthelot, D.; Zaja, M.; Brone, B.; Geuens, I.; Mercken, M. Analogues of morphanthridine and the tear gas dibenz[b,f ][1,4]oxazepine (CR) as extremely potent activators of the human transient receptor potential ankyrin 1 (TRPA1) Channel. *J. Med. Chem.* **2010**, *53*, 7011–7020.

(30) Nagatomo, K; Kubo, Y.; Caffeine activates mouse TRPA1 channels but suppresses human TRPA1 channels. *Proc. Nat. Acad. Sci.* **2008**, *105*, 17373-17378.

(31) Klionsky, L.; Tamir, R.; Gao, B.; Wang, W.; Immke, D. C.; Nishimura, N.; Gavva, N. R.; Species-specific pharmacology of Trichloro(sulfanyl)ethyl benzamides as transient receptor potential ankyrin 1 (TRPA1) antagonists. *Mol. Pain* **2007**, *3*, 39.

(32) Nash, M.S.; McIntyre, P.; Groarke, A.; Lilley, E.; Culshaw, A.; Hallett, A.; Panesar, M.; Fox, A.; Bevan, S. 7-tert-Butyl-6-(4-chloro-phenyl)-2-thioxo-2,3-dihydro-1H-pyrido[2,3-d]pyrimidin-4-one, a classic polymodal inhibitor of transient receptor potential vanilloid type 1 with a reduced liability for hyperthermia, is analgesic and ameliorates visceral hypersensitivity. *J. Pharmacol. Exp. Ther.* **2012**, *342*, 389-98.

(33) Walker, K. M.; Urban, L.; Medhurst, S. J.; Patel, S.; Panesar, M.; Fox, A. J.; McIntyre, P. The VR1 antagonist capsazepine reverses mechanical hyperalgesia in models of inflammatory and neuropathic pain. *J. Pharmacol. Exp. Ther.* **2003**, *304*, 52-56.

(34) Sandkühler, J. Models and mechanisms of hyperalgesia and allodynia. *Physiol. Rev.* **2009**, *89*, 707–758.

(35) Laird, J. M.; Martinez-Caro, L.; Garcia-Nicas, E.; Cervero F. A new model of visceral pain and referred hyperalgesia in the mouse. *Pain* **2001**, *92*, 335-342.

(36) Gavva, N. R. Body-temperature maintenance as the predominant function of the vanilloid receptor TRPV1. *Trends Pharmacol. Sci.* **2008**, *29*, 550-557.

(37) Gavva, N. R.; Treanor, J. J.; Garami, A.; Fang, L.; Surapaneni, S.; Akrami, A.; Alvarez, F.; Bak, A.; Darling, M.; Gore, A.; Jang, G. R.; Kesslak, J. P.; Ni, L.; Norman, M. H.; Palluconi,

G.; Rose, M. J.; Salfi, M.; Tan, E.; Romanovsky, A. A.; Banfield, C.; Davar G. Pharmacological blockade of the vanilloid receptor TRPV1 elicits marked hyperthermia in humans. *Pain* **2008**, *136*, 202-210.

(38) Hertzberg, U.; Eliav, E.; Bennett, G. J.; Kopin, I. J. The analgesic effects of R(+)-WIN 55,212-2 mesylate, a high affinity cannabinoid agonist, in a rat model of neuropathic pain. *Neurosci. Lett.* **1997**, *221*, 157-160.

(39) Li, C.; Liu, B.; Chang, J.; Groessl, T.; Zimmerman, M.; He, Y.; Isbell, J.; Tuntland, T.; A modern *in vivo* pharmacokinetic paradigm: combining snapshot, rapid, and full PK approaches to optimize and expedite early drug discovery. *Drug Discov. Today* **2013**, *18*, 71-78.

**Scheme 1.** Synthetic route to 5-arylindazoles [a]

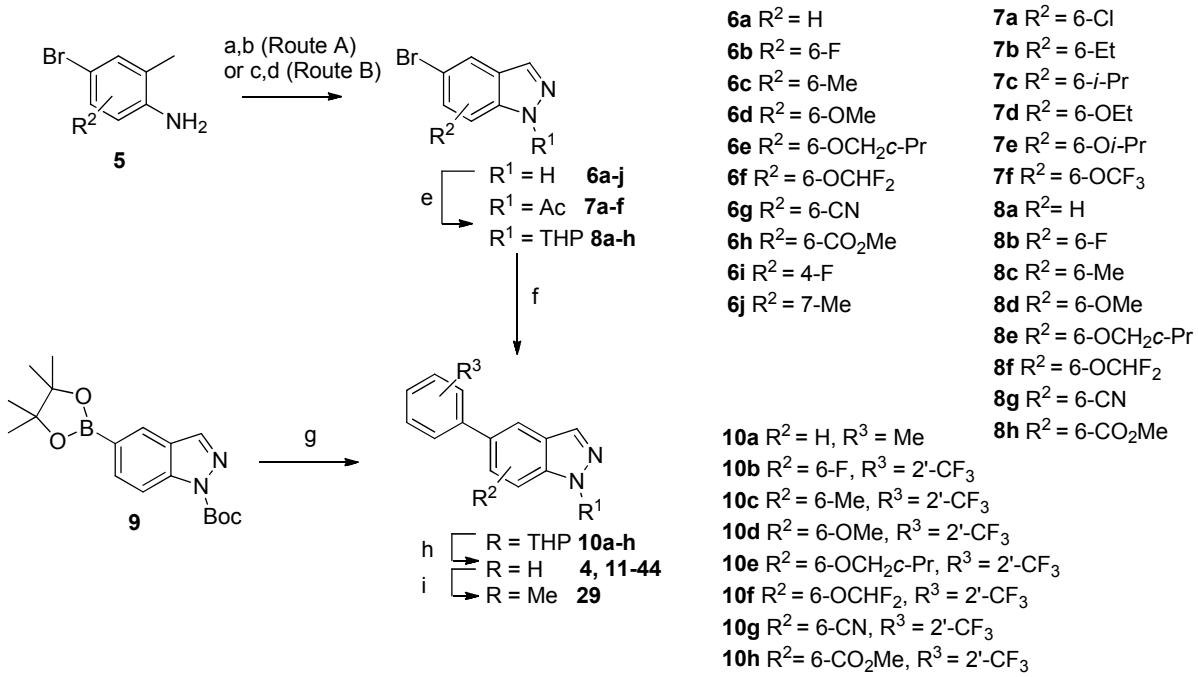


[a]Reagents and conditions: a) acetic anhydride, toluene, 120 °C; b) acetic anhydride, KOAc, 18-crown-6, *iso*-amyl nitrite, $CHCl_3$, 55 °C; c) *t*-BuONO, $BF_3$•$Et_2O$, $CH_2Cl_2$; d) KOAc, 18-crown-6, $CH_2Cl_2$; e) *p*-TsOH, 2,3-dihydropyran, $CHCl_3$, rt; (f) boronic acid, $Cs_2CO_3$, $Pd(PPh_3)_4$, dioxane, $H_2O$, 120 °C, microwave; or boronic acid, $Cs_2CO_3$, chloro(di-2-norbornylphosphino)(2'-dimethylamino-1,1'-biphenyl-2-yl)palladium (II), dioxane/$H_2O$, 160 °C, microwave; rt; g) $Na_2CO_3$, $Pd(PPh_3)_4$, aryl bromide, EtOH/$H_2O$, 120 °C, microwave; h) HCl (4M in dioxane), MeOH, rt; i) NaH, MeI, DMF, rt.

**Scheme 2.** Synthesis of **35**, **40** and **44**[a]

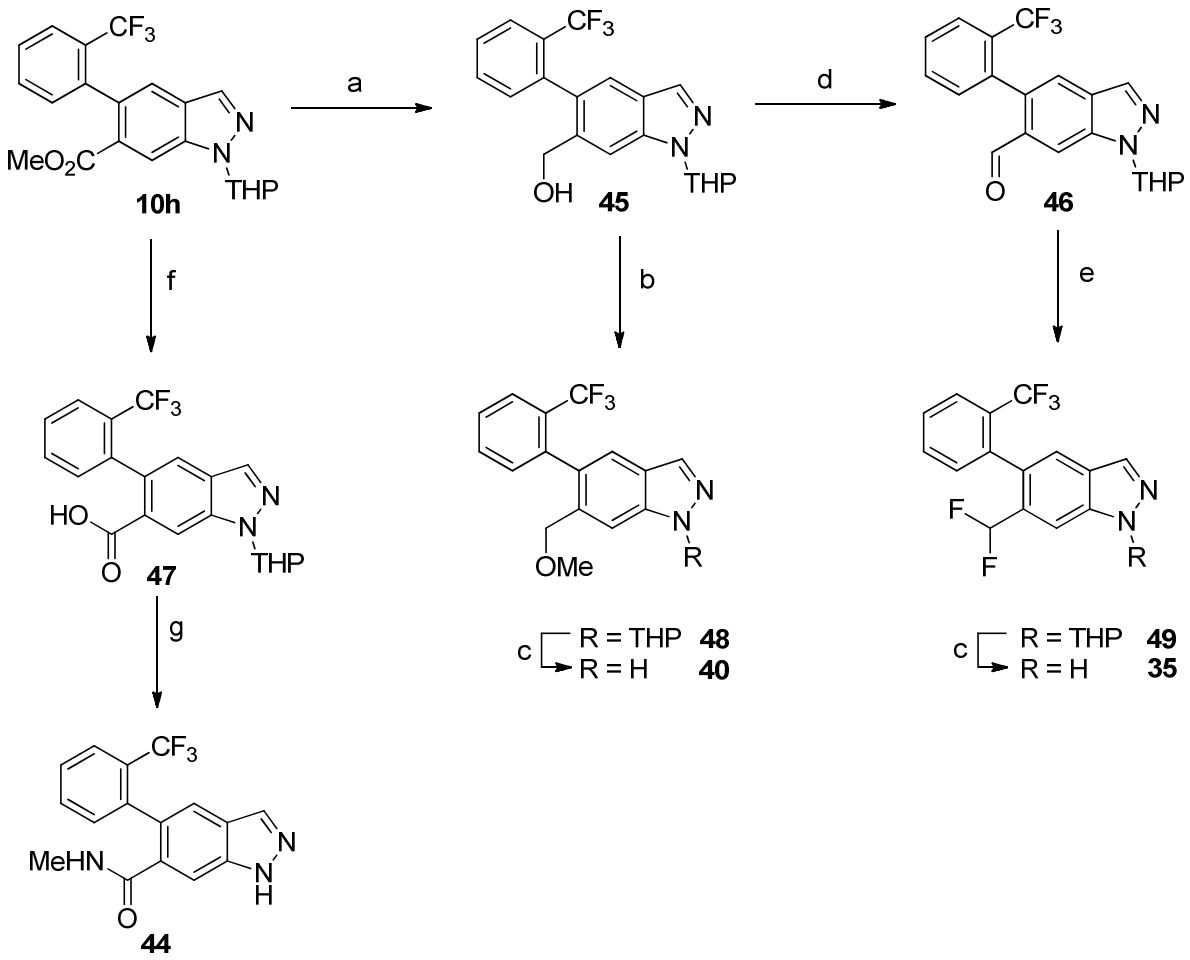


[a]Reagents and conditions: a) $LiAlH_4$, THF, 0°C to rt, 69%; b) NaH, MeI, DMF, 94%; c) HCl (4M in dioxane), MeOH, rt to 50°C, 37-76%; d) $MnO_2$, $CH_2Cl_2$, rt, 62%; e) DAST, $CH_2Cl_2$, reflux, 45%; f) NaOH, THF, MeOH, $H_2O$; g) $SOCl_2$, toluene, 70 °C then DIPEA, methylamine, 70 °C, 22%.

**Scheme 3.** Synthesis of **34** [a]

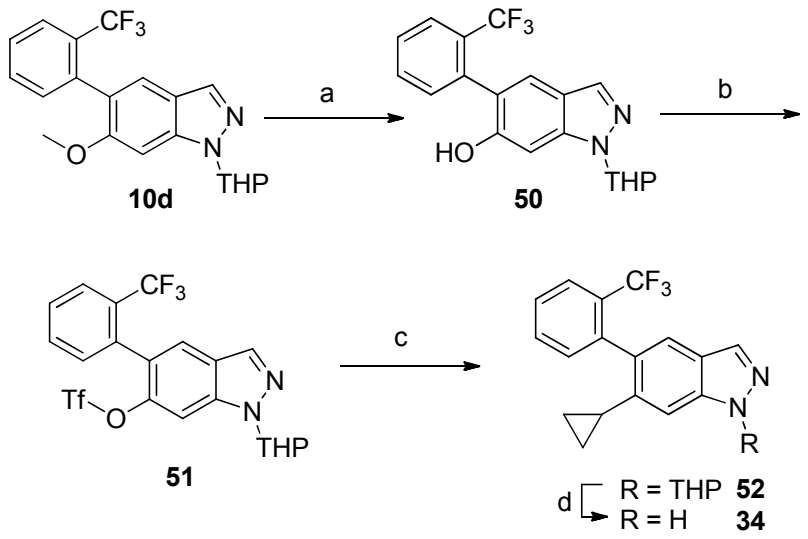


[a]Reagents and conditions: a) 1-dodecanethiol, NaOH, NMP, 130 °C, 96%; b) N-phenyltriflimide, $K_2CO_3$, THF, 120 °C, 77%; c) c-PrB(OH)$_2$, Pd(PPh$_3$)$_4$, dioxane, $H_2O$, microwave, 100 °C, 68%; d) HCl (4M in dioxane), MeOH, rt, 38%.

**Table 1**. SAR of the 2-substituent on the Phenyl Ring

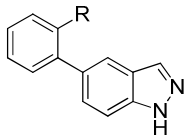


| Compound | R | **hTRPA1 $IC_{50}$ ± SD (μM) (%inhibition)** |
|---|---|---|
| 4 | Cl | 1.23 ± 0.49 (91%) |
| 11 | H | >30 |
| 12 | F | 3.95 ± 1.7 (68%) |
| 13 | methyl | 7.81 ± 0.64 (78%) |
| 14 | ethyl | 0.584 ± 0.19 (96%) |
| 15 | *iso*-propyl | 0.514 ± 0.067 (93%) |
| 16 | *tert*-butyl | 3.40 ± 0.40 (96%) |
| 17 | $CF_3$ | 0.164 ± 0.049 (98%) |
| 18 | $CHF_2$ | 2.20 ± 0.40 (93%) |
| 19 | $OCF_3$ | 3.43 ± 0.62 (97%) |
| 20 | CN | 1.29 ± 0.19 (91%) |

**Table 2.** SAR for Substitution Around the 5-Phenylindazole

| Compound | Structure | hTRPA1 $IC_{50}$ ± SD (μM) (%inhibition) |
|---|---|---|
| 21 | 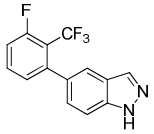 | 8.90 ± 0.90 (97%) |
| 22 | 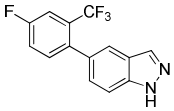 | >30 |
| 23 | 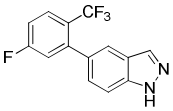 | 0.306 ± 0.11 (98%) |
| 24 | 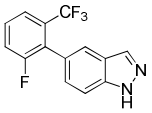 | 1.23 ± 0.20 (95%) |
| 25 | 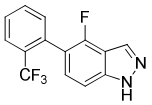 | 0.296 ± 0.019 (97%) |
| 26 | 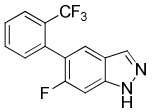 | 0.048 ± 0.001 (98%) |
| 27 | 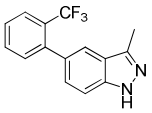 | 3.09 ± 3.5 (83%) |
| 28 | 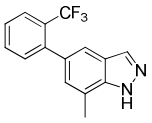 | 6.72 ± 1.6 (98%) |
| 29 | 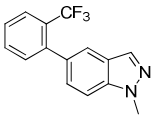 | 7.41 ± 0.5 (98%) |

**Table 3**. Activity of the 6-Substituted 5-(Trifluoromethylphenyl)indazoles

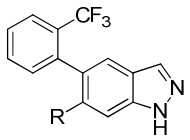


| Compound | R | hTRPA1 $IC_{50}$ ± SD (μM) (%inhibition) |
|---|---|---|
| 26 | F | 0.043 ± 0.011 (98%) |
| 30 | Cl | 0.024 ± 0.003 (98%) |
| 31 | Me | 0.015 ± 0.004 (99%) |
| 32 | Et | 0.050 ± 0.021 (100%) |
| 33 | *iso*-Pr | 25.4 ± 0.90 (59%) |
| 34 | *cyclo*-Pr | 0.061 ± 0.013 (99%) |
| 35 | $CHF_2$ | 0.103 ± 0.042 (100%) |
| 36 | OMe | 0.026 ± 0.003 (98%) |
| 37 | OEt | 0.039 ± 0.005 (97%) |
| 38 | O-*iso*-Pr | 0.970 ± 0.19 (97%) |
| 39 | $OCH_2$-cycloPr | 0.026 ± 0.009 (98%) |
| 40 | $CH_2OMe$ | 0.142 ± 0.011 (97%) |
| 41 | $OCF_3$ | 0.036 ± 0.021 (99%) |
| 42 | $OCHF_2$ | 0.050 ± 0.024 (98%) |
| 43 | CN | 0.129 ± 0.029 (100%) |
| 44 | C(O)NHMe | >30 |

**Table 4.** Inhibition of TRPA1 Activation by Different Chemical Agonists

| Entry | hTRPA1-CHO cinnamaldehyde agonist $IC_{50}$(μM) (%inhibition) | hTRPA1-CHO allyl isothiocyanate agonist $IC_{50}$(μM) (%inhibition) | hTRPA1-CHO dibenzo[b,f][1,4]oxazepine-4-carboxamide agonist $IC_{50}$(μM) (%inhibition) |
|---|---|---|---|
| **17** | 0.164 (99%) | 0.084 (97%) | 0.550 (100%) |
| **31** | 0.015 (99%) | 0.018 (99%) | 0.020 (100%) |

**Table 5.** Species cross-reactivity and TRP channel selectivity data for Compounds **17, 30, 31, 41, 36** and **39**

| **Entry** | **hTRPA1 $IC_{50}$ ± SD (μM) (%inhibition)** | **rTRPA1 $IC_{50}$ ± SD (μM) (%inhibition)** | **mTRPA1 $IC_{50}$ ± SD (μM) (%inhibition)** | **hTRPV1 $IC_{50}$ ± SD (μM) (%inhibition)** | **hTRPV3 $IC_{50}$(μM) (%inhibition)** | **hTRPM8 $IC_{50}$ ± SD (μM) (%inhibition)** |
|---|---|---|---|---|---|---|
| **17** | 0.164 ± 0.049 (99%) | 0.400 ± 0.140 (98%) | 0.252 ± 0.083 (100%) | > 30 (34%) | > 30 (10%) | 9.0 ± 3 (95%) |
| **30** | 0.024 ± 0.003 (98%) | 0.169 ± 0.018 (98%) | 0.094 ± 0.006 (100%) | 16.7 ± 1.2 (70%) | > 30 (0%) | 17.1 ± 1.7 (71%) |
| **31** | 0.015 ± 0.004 (99%) | 0.089 ± 0.013 (99%) | 0.053 ± 0.005 (100%) | 5.1 ± 0.40 (87%) | > 30 (0%) | 9.2 ± 0.9 (90%) |
| **41** | 0.036 ± 0.021 (99%) | 0.627 ± 0.022 (100%) | 0.254 ± 0.045 (100%) | 11.5 ± 2.0 (78%) | > 30 (22%) | 6.4 ± 2.1 (100%) |
| **36** | 0.026 ± 0.003 (98%) | 0.099 ± 0.019 (99%) | 0.161 ± 0.028 (100%) | > 30 (35%) | > 30 (35%) | 10.9 ± 0.9 (100%) |
| **39** | 0.026 ± 0.009 (98%) | 0.190 ± 0.029 (99%) | 0.104 ± 0.007 (100%) | 8.1 ± 1.30 (99%) | > 30 (5%) | 4.40 ± 0.5 (100%) |

**Table 6.** Pharmacokinetic assessment of Selected Analogues in Rat following Intravenous and Oral Administration

| Dosing route (Wistar rats) | **Intravenous** | | | | **Oral Administration (10 mg/kg) vehicle: 0.5%MC/0.5%Tween80, suspension** | | | |
|---|---|---|---|---|---|---|---|---|
| Compound | IV (dose); vehicle | CL (mL/min/kg) | Vss (L/kg) | $T_{1/2}$ (h) | AUC (h*nM) | $C_{max}$ (nM) | $T_{max}$ (h) | F (%) |
| **17**[i] | a | 14.7 | 2.06 | 3.5 | 15736 | 4769 | 0.5 | 37 |
| **30** | a | 13.6 ± 1.4 | 1.65 ± 0.31 | 3.4 ± 0.5 | 26170 ± 1639 | 6049 ± 1302 | 0.5 | 63 ± 4 |
| **31** | b | 25.7 ± 2.9 | 2.39 ± 0.19 | 4.3 ± 0.4 | 9309 ± 1048 | 3531 ± 597 | 0.5 | 39 ± 4 |
| **36** | c | 35.5 ± 3.0 | 3.60 ± 0.3 | 6.6 ± 1.0 | 8200 ± 4900 | 2001 ± 1308 | 0.8 | 50 ± 29 |
| **39**[i] | a | 50.0 | 3.33 | 1.1 | 384 | 98 | 1.0 | 4 |

[a] IV (3 mg/kg) vehicle: 75%PEG300:25%D5W, solution; [b]IV (5 mg/kg) vehicle 2.5 mg/mL in 10% EtOH /30%PEG300 /60% solutol (10% solution); [c]IV (1 mg/kg) vehicle: 75%PEG200:25%D5W, solution.

[i] Rapid PK data[39]

**Table 7.** Pharmacokinetic assessment of **31** in Mouse following Intravenous and Oral Administration

| Dosing route (Balb C mice) | **IV (5 mg/kg) vehicle: 2.5 mg/mL in 10% EtOH /30%PEG300 /60% solutol ( 10% solution)** | | | **PO (20 mg/kg) vehicle: 0.5%MC/0.5%Tween80, suspension** | | | |
|---|---|---|---|---|---|---|---|
| Compound | CL (mL/min/kg) | Vss (L/kg) | $T_{1/2}$ (h) | AUC (h*nM) | $C_{max}$ (nM) | $T_{max}$ (h) | F (%) |
| **31** | 39.3 ± 13.8 | 4.07 ± 1.93 | 3.64 ± 1.57 | 5595 ± 1983 | 1272 ± 90 | 0.5 | 17 ± 5.9 |

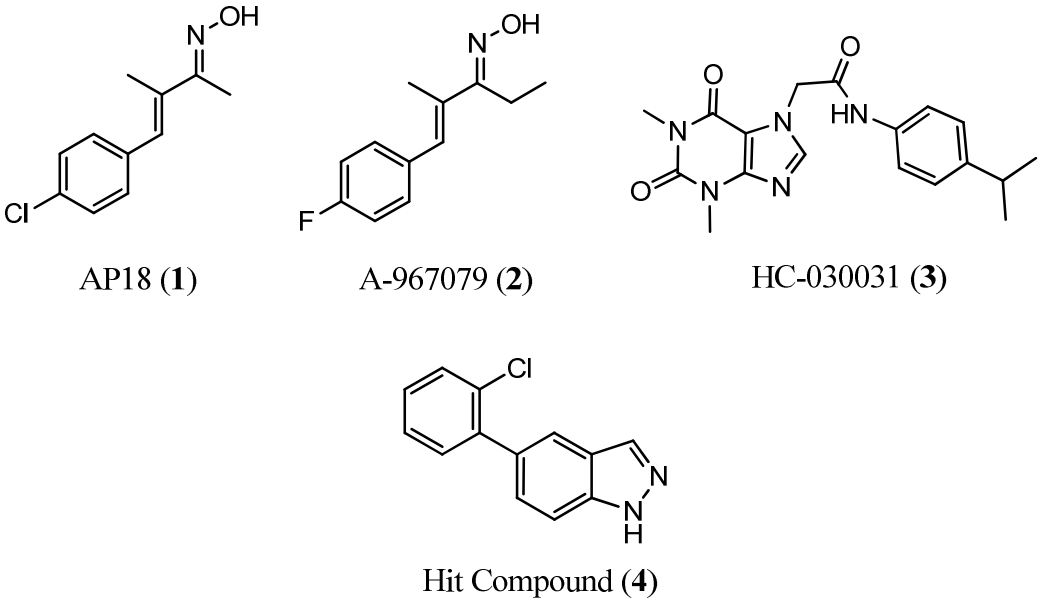


**Figure 1**. Antagonists of TRPA1 reported in the literature and Hit Compound **4**

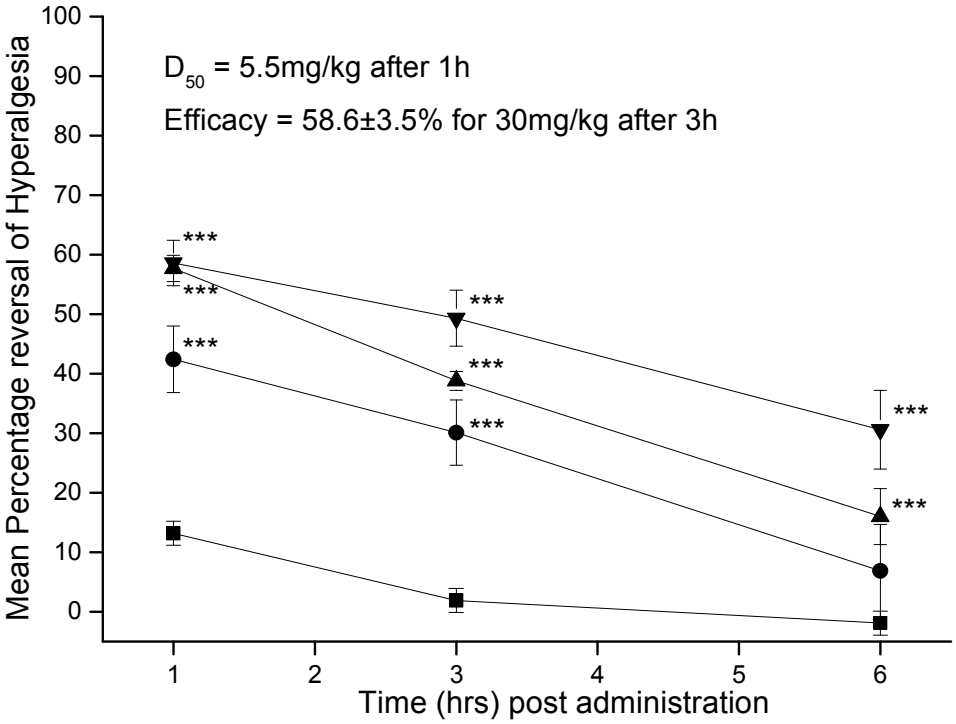


**Figure 2**. Reversal of FCA-induced mechanical hyperalgesia in rats by the TRPA1 antagonist **31**. Data are mean ± S.E.M for vehicle (■), 3 (●), 10 (▲) and 30 (▼) mg/kg **31** p.o. with

***P<0.001 using one-way ANOVA followed by Dunnett's test compared to vehicle group; *n* = 6 rats/dose.

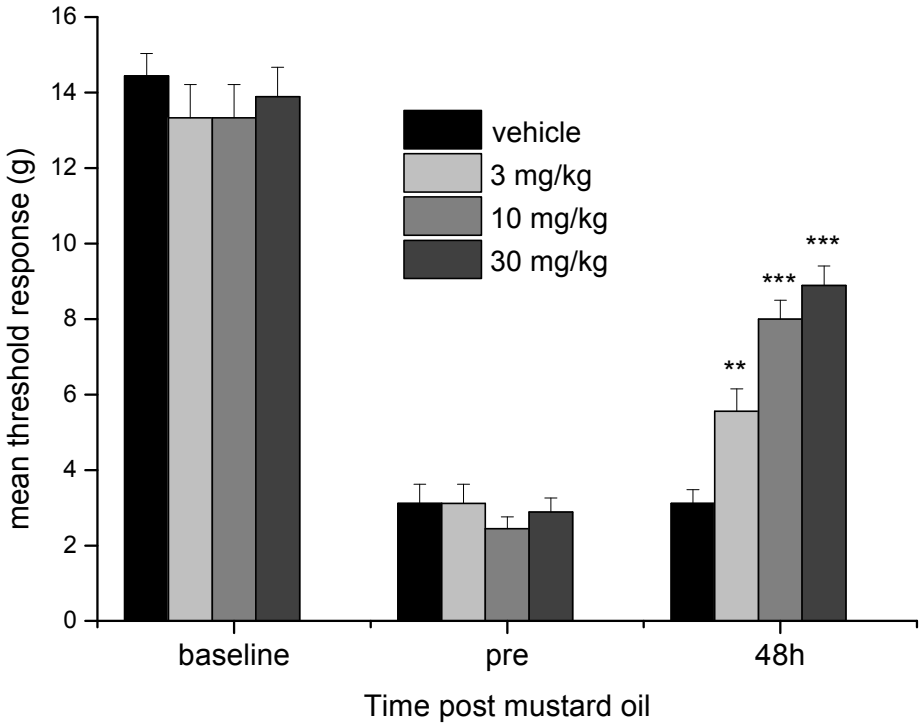


**Figure 3.** Reversal of established mustard-induced allodynia in mice by the TRPA1 antagonist **31**. Data are mean ± S.E.M with *** P<0.001 and ** P<0.01 using one-way ANOVA followed by Dunnett's test compared to vehicle group; *n* = 6 mice/dose.

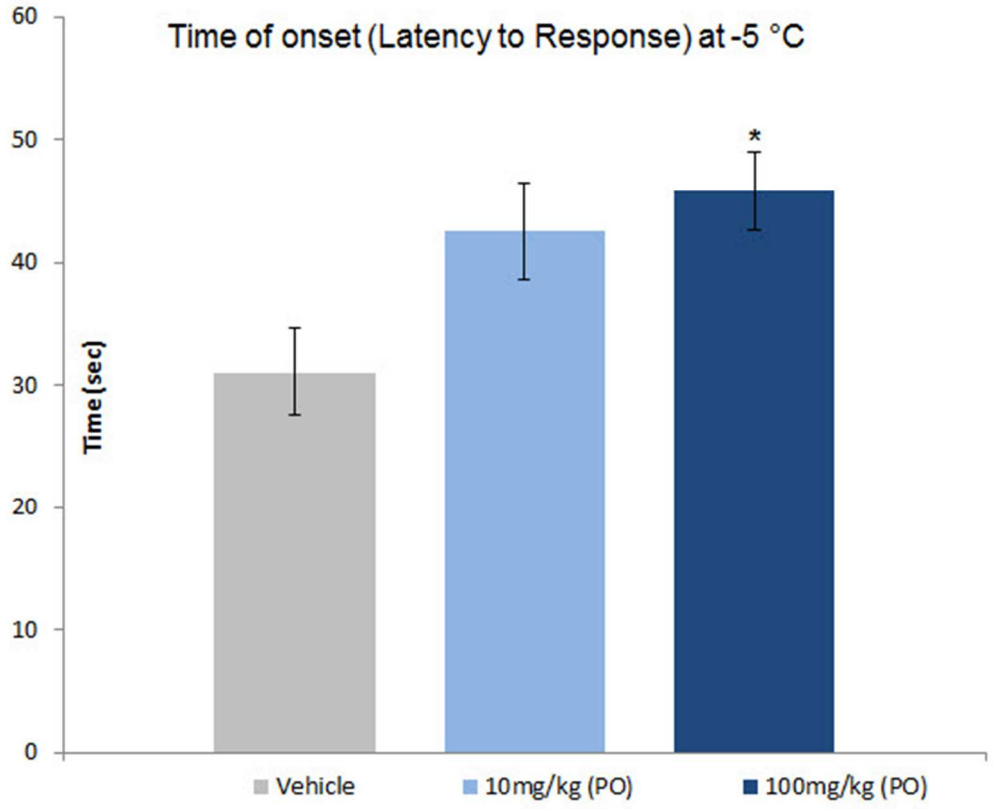


**Figure 4.** Effect of the TRPA1 antagonist **31** on thermosensation in naive mice when placed upon a cold (-5 °C) surface. Data are mean ± S.E.M with * P<0.05 using one-way ANOVA followed by Dunnett's test compared to vehicle group; *n* = 7 mice/dose

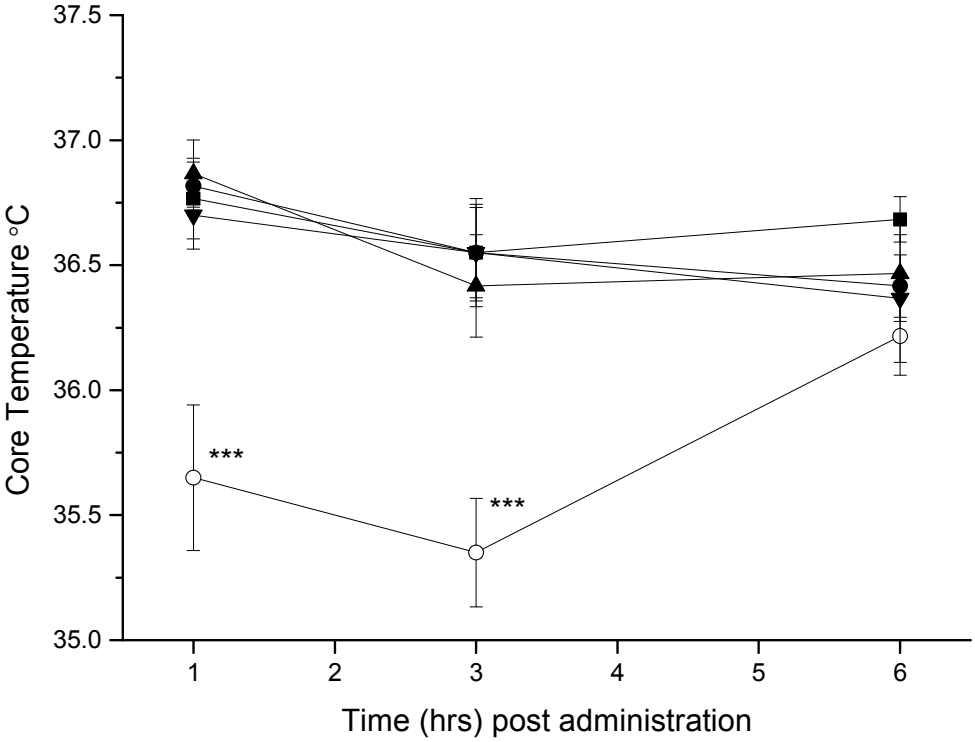


**Figure 5.** The TRPA1 antagonist **31** has no effect on core body temperature in contrast to the cannabinoid receptor agonist WIN55,212-2. Data are mean ± S.E.M for vehicle (■), 10 (●), 30 (▲) and 100 (▼) mg/kg **31** *p.o.* and 6mg/kg for WIN55,212-2 (○) *s.c.* with *** P<0.001 using one-way ANOVA followed by Dunnett's test compared to vehicle group; $n$ = 6 rats/dose.

Table of Contents graphic

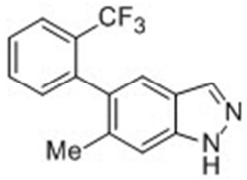


**TRPA1 Antagonist**
**Compound 31**
hTRPA1 $IC_{50}$ = 0.015 μM
rTRPA1 $IC_{50}$ = 0.085 μM

Rat Mechanical Hyperalgesia
$D_{50}$ = 5.5 mg/kg at 1hr